Marika Eerikäinen

DNA origami-based enzyme nanoreactor

School of Electrical Engineering

Thesis submitted for examination for the degree of Master of Science in Technology.

Espoo 24.11.2014

Thesis supervisor:

Prof. Mauri Kostiainen

Thesis advisor:

Ph.D. Veikko Linko

Aalto University
School of Electrical
Engineering

AALTO UNIVERSITY
SCHOOL OF ELECTRICAL ENGINEERING

ABSTRACT OF THE
MASTER'S THESIS

Author: Marika Eerikäinen

Title: DNA origami-based enzyme nanoreactor

Date: 24.11.2014 Language: English Number of pages: 6+42

Department of biotechnology and chemical technology

Professorship: Polymer technology Code: Kem-100

Supervisor: Prof. Mauri Kostiainen

Advisor: Ph.D. Veikko Linko

In this thesis the concept of DNA origami and enzyme nanoreactor is introduced. A modular enzymatic DNA origami nanoreactor is designed and assembled and the successfull folding is confirmed with agarose gel electrophoresis and transmission electron microscopy images. The nanoreactor consists of two monomer origamis, one equipped with glucose oxidase (GOx) enzyme and one with horseradish peroxidase (HRP) enzyme. The attachment is accomplished using non-covalent but strong biotin-avidin binding. In proof-of-concept experiments first the activity of individual monomer units is examined measuring the change of concentration of reporter agent tetramethylbenzidine diimine (TMB*) with UV-Vis spectrophotometry. Next the dimer origamis are formed from two monomer units and finally the efficient GOx/HRP enzyme-pair cascade reaction is demonstrated. The reactor could be utilised as a nanoscale diagnostic tool, and modularity of the proposed system would further enable more complex reactions.

Keywords: DNA origami, horseradish peroxidase, glucose oxidase, nanoreactor, enzyme cascade, DNA nanotechnology

AALTO-YLIOPISTO
SÄHKÖTEKNIIKAN KORKEAKOULU

DIPLOMITYÖN
TIIVISTELMÄ

Tekijä: Marika Eerikäinen

Työn nimi: DNA origami -pohjainen entsyyminanoreaktori

Päivämäärä: 24.11.2014 Kieli: Englanti Sivumäärä: 6+42

Biotekniikan ja kemian tekniikan laitos

Professuuri: Polymeeriteknologia Koodi: Kem-100

Valvoja: Prof. Mauri Kostiainen

Ohjaaja: FT Veikko Linko

Tämä diplmomityö käsittelee DNA origamin teoriaa, valmistusta sekä sovelluksia. Tutkimusosiossa suunnitellaan ja valmistetaan DNA origami -tekniikalla entsymaattinen nanoreaktori. Prosessin onnistuminen ja DNA origamien korkea saanto varmistetaan agaroosigeelielektroforeesilla sekä läpäisyelektronimikroskooppikuvilla. Nanoreaktori muodostetaan kahdesta monomeeriyksiköstä, joista toinen sisältää glukoosioksidaasientsyymin (GOx) ja toinen piparjuurioksidaasientsyymin (HRP). Entsyymien kiinnitysmenetelmänä käytetään eikovalenttista, mutta silti vahvaa biotiini-avidiinisidosta. Ennen dimeerin kokoamista, yksittäisten monomeerituubien entsyymiaktiivisuus mitataan detektoimalla reportterina toimivan tetrametyylibenzidiinin di-imiinin (TMB*) konsentraation muutosta UV/Vis spektrofotometrialla. Seuraavaksi muodostetaan dimeeri liittämällä kaksi monomeerituubia yhteen ja lopulta demonstroidaan GOx/HRP -entsyymiparin kaskadireaktio nanoreaktorin sisällä. Esiteltyä reaktoria voidaan tulevaisuudessa hyödyntää erilaisina nanomittakaavan diagnostiikkatyökaluina ja DNA origamituubien modulaarisuus mahdollistaa myös monimutkaisemmat katalyysireaktiosarjat.

Avainsanat: DNA origami, piparjuuriperoksidaasi, glukoosioksidaasi, nanoreaktori, entsyymikaskadi, DNA nanoteknologia

Preface

I would like to thank my advisor Dr. Veikko Linko for the patient and proficient guidance throughout this project and Prof. Mauri Kostiainen for the opportunity to learn and explore this amazing field of DNA nanotechnology.

Otaniemi, 24.11.2014

Marika Eerikäinen

Contents

Symbols and abbreviations

Abbreviations

ABTS	2,2'-azino-bis(3-ethylbenzothiazoline-6-sulphonic acid)
AFM	atomic force microscopy
b-GOx	biotinylated glucose oxidase
b-HRP	biotinylated horseradish peroxidase
bp	base pair
CalB	*Candida antarctica* lipase B
CpG	cytosine-phosphate-guanine
DMSO	dimethyl sulfoxide
DNA	deoxyribonucleic acid
dsDNA	double stranded DNA
EDTA	ethylenediaminetetraacetic acid
FRET	fluorescence resonance energy transfer
GOx	glucose oxidase
G4	G-quadruplex
HRP	horseradish peroxidase
IgG	immunoglobulin G
kD, kDa	kilo dalton
NMR	nuclear magnetic resonance
nt	nucleotide
NTV	neutravidin
ODN	oligodeoxynucleotides
PBS	phosphate buffered saline
PCR	polymer chain reaction
PEG	poly(ethylene glycol)
rcf	relative centrifugal force
RNA	ribonucleic acid
ssDNA	single stranded DNA
TAE	tris-acetate-EDTA
TEM	transmission electron microscope
TLR	Toll-like receptor
TMB	tetramethylbenzidine
TMB*	tetramethylbenzidine diimine
Tris	tris(hydroxymethyl)aminomethane
UV/Vis	ultraviolet/visible (spectrophotometry)
2D	two-dimensional
3D	three-dimensional

1 Introduction

The field of DNA nanotechnology aims to create artificial nanostructures out of nucleic acids for various technological uses. The nucleic acids are not executing their original task as carriers of genetic information in living cells, but rather acting as engineering material and building blocks. DNA nanotechnology utilises the self-assembly of DNA and nucleic acids resulting from the well understood but still strict rules of base pairing. It enables the producing of precisely designed and controllable complex structures in nanometre scale.

Nadrian Seeman was the first to publish the idea of using DNA as a building material in the early 1980s. The first assemblies were linear and one-dimensional. Method development allowed first production of flexible branched junction structures and topological structures and later crossover DNA tiles with greater rigidity. Single stranded overhangs, called sticky ends, allowed interstructure associations [1]. In 2006 Paul Rothemund developed a method called DNA origami in which a long single stranded viral DNA is folded into a desired shape by multiple short strands called staple strands. The method was a milestone for DNA nanotechnology since it enabled the relatively straightforward production of nanoscale size-limited and uniform 2D and 3D structures for the first time [2]. In this thesis the term DNA origami is used to refer to Rothemund's method.

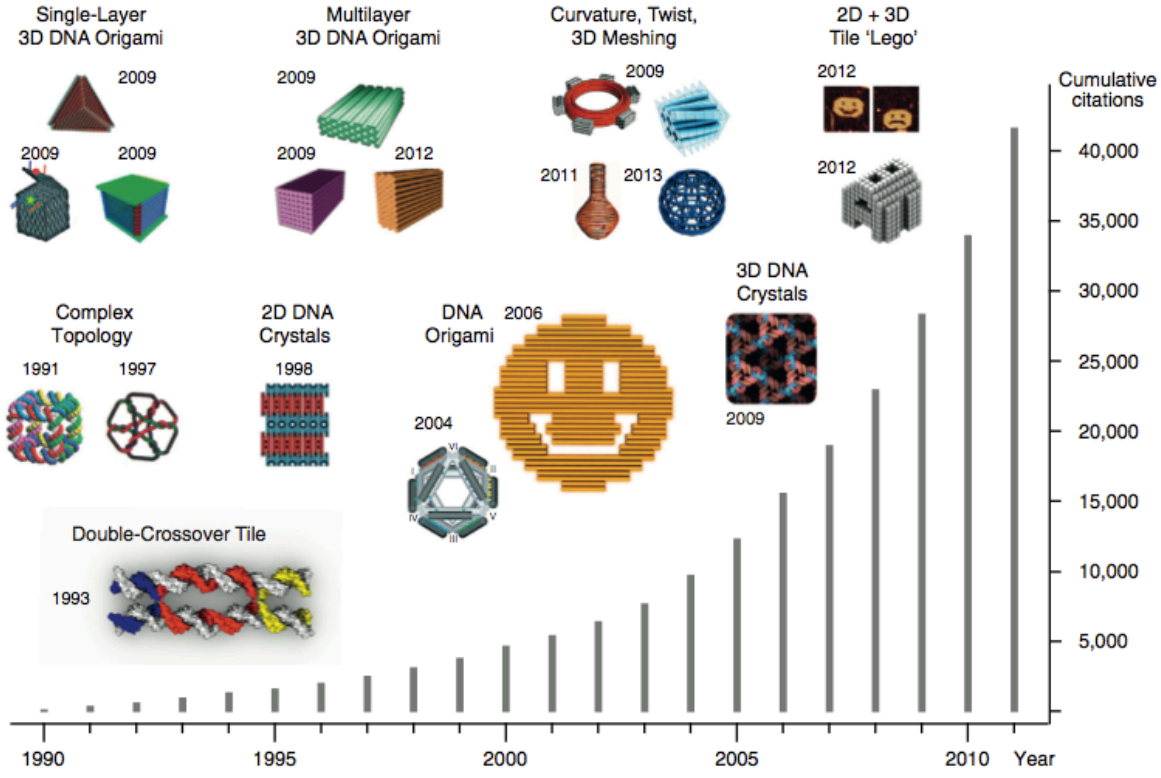

Figure 1: Collection of DNA nanotechnology structures and a histogram of cumulative citations illustrating the growth of interest in the field [3].

In figure 1 there is a collection of DNA structures shown with the year they were first published. In the bottom panel the histogram shows the cumulative citations about the field of DNA nanotechnology [3]. To date, the smallest reported DNA-based structure is a DNA prism built out of a single DNA strand with a characteristic dimension of 3.4 nm. Also, DNA wireframe structures with radii of 50–100 nm, DNA containers with edges up to 55 nm, DNA brick crystals with lateral dimensions up to micrometre size [4] and DNA nanotubes with axial dimensions over 10 µm have been constructed [5].

In this thesis project a hollow hexagonal DNA origami tube is designed and produced and an enzymatic cascade reaction inside two origami tubes attached together forming a synthetic nanoreactor is demonstrated. In chapter 2 the basic properties of DNA as a building material are reviewed and in chapter 3 the concept of DNA origami is introduced, also some applications are listed and discussed. The materials and methods of the research are described in chapter 4 and finally the results are shown in chapter 5.

2 Deoxyribonucleic acid as a building material

Deoxyribonucleic acid, DNA, is an attractive building material for nanostructures that require precise programmability and control over spatial arrangement. DNA possesses extraordinary combination of properties including sequence programmability, specific molecular recognition, the rigidity of the double helix, sequence-independent nanoscale structure, commercial availability due to automated synthesis, versatile chemical modifications and the ability of enzymatic scission and ligation. These features make DNA one of the most promising molecules to organise various functional nano-sized objects such as proteins, drug molecules or metal nanoparticles [6]. The structure of DNA was discovered by James Watson and Francis Crick in 1953 and it is described in the following chapter [7, p. 332].

2.1 Structure of DNA

Nucleic acids are long threadlike polymers that are made up of a linear compilation of nucleotides. Nucleotides are the phosphate esters of nucleosides. All nucleotides are constructed from a nitrogen heterocyclic base, a pentose sugar and a phosphate residue [8, p. 14–23]. Since the phosphate groups (PO_4^-) in the backbone are negatively charged at pH 7, like shown in figure 2b, all DNA strands bear a negative charge [9], [7, p. 325–362]. Nucleic acids are soluble in water and their solutions are quite viscous [8, p. 14–23]. The size of a nucleic acid varies a lot and it is typically described as the number of base pairs (bp). For example a transfer RNA (tRNA) molecule has approximately 80 nucleotides while an eukaryotic chromosome can have over 10^8 nucleotide pairs. The genomic DNA in a human cell has 3900 Mbp and is approximately 990 mm long.

In the primary structure of DNA (figure 2b) each nucleoside is joined by a phosphate diester from its 5′-hydroxyl group to the 3′-hydroxyl group of one neighbour and by a second phosphate diester from its 3′-hydroxyl group to the 5′-hydroxyl group of its other neighbor. In other words, there are no 5′-5′ or 3′-3′ linkages in a normal DNA primary structure [10]. A DNA sequence refers to the bases in a strand listed starting from the 5′-end [9].

Two strands of DNA with complementary base sequences can form a secondary structure of DNA, the DNA double-helix. In a double-helix the two single strands run to opposite directions like shown in figure 2c. Base pairing is based on hydrogen bonding also known as Watson-Crick pairing and it allows the DNA helix to maintain its helical form independent of the nucleotide sequence. A base pair is formed by guanine (G) and cytosine (C) or by adenine (A) and thymine (T). The G-C pair is formed by three hydrogen bonds with the energy of E_{G-C}=16.79 kcal/mol and the A-T pair with two hydrogen bonds and energy of E_{A-T}=7.00 kcal/mol. Also other pairs can be formed and other pairing patterns exist, for instance Hoogsteen pairs and Crick "wobble" pairs, but the above mentioned Watson-Crick pairing and A-T and G-C pairs are energetically the most favourable ones [8, p. 14–55]. In addition to hydrogen bonding, the stability of the double-helix results also from the base stacking, the weak van der Waals and dipole-dipole interactions between

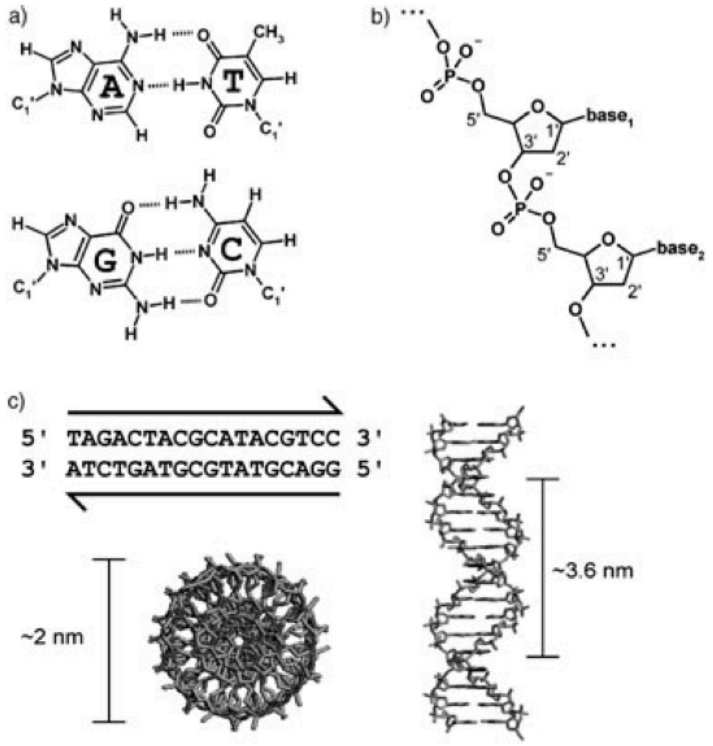

Figure 2: a) The base pair between adenosine and thymine is formed by two hydrogen bonds and between guanine and cytosine by three hydrogen bonds. b) The backbone of a DNA strand is formed by alternating pentose sugars and phosphate residues and it bears a negative charge. c) Complementary strands run to opposite directions. Hydrophilic backbones of alternating deoxyribose and phosphate groups face outwards from the structure. The bases of both strands of the double helix are stacked inside and their hydrophobic, nearly planar ring structures very close together and perpendicular to the main axis. This arrangement results as the alternating minor and major grooves [7, 11].

the bases. Corresponding energy values for stacking interactions are 14.59 kcal/mol for G-C pair and 3.82 kcal/mol for A-T pair. Compared to covalent bonds (for example between two carbon atoms E_{C-C}=83.1 kcal/mol) the interactions within a DNA helix are still relatively weak. Thereby the hybridisation of DNA strands is reversible and the strands can be separated, for example, by heating [9].

DNA can adapt different conformations as a secondary structure. The three most common conformations are A-DNA, B-DNA and Z-DNA. At low humidity and high salt concentration, the most favoured form is A-DNA. At high humidity and low salt concentration, the more probable form is B-DNA [8, p. 24–33]. B-form of DNA is the most stable and common in physiological conditions. The diameter of the helix is approximately 2 nm and it has an average of 10.5 base pairs per helical turn while the diameter of a A-DNA helix is 2.6 nm and it has 11 bp per turn. A- and B-DNA being right-handed the Z-DNA is left-handed and has 12 bp per turn. The structural differences are the reason behind the varying stabilities in

different solutions as well as their electronic properties [12, 13, 14]. All the three structures are illustrated in figure 3 [15]. Also more uncommon structures have been discovered, like triple-stranded H-DNA and four-stranded G4-structures. The G4-structure, also known as G-guadruplex, G-tetrad or G_4-DNA, can be found, for instance, in telomeres in human chromosomes [8, p. 14–55]. The structure has been studied especially for its curious electronic properties suggesting it to be adaptable for nanowires or other molecular electronics applications [16].

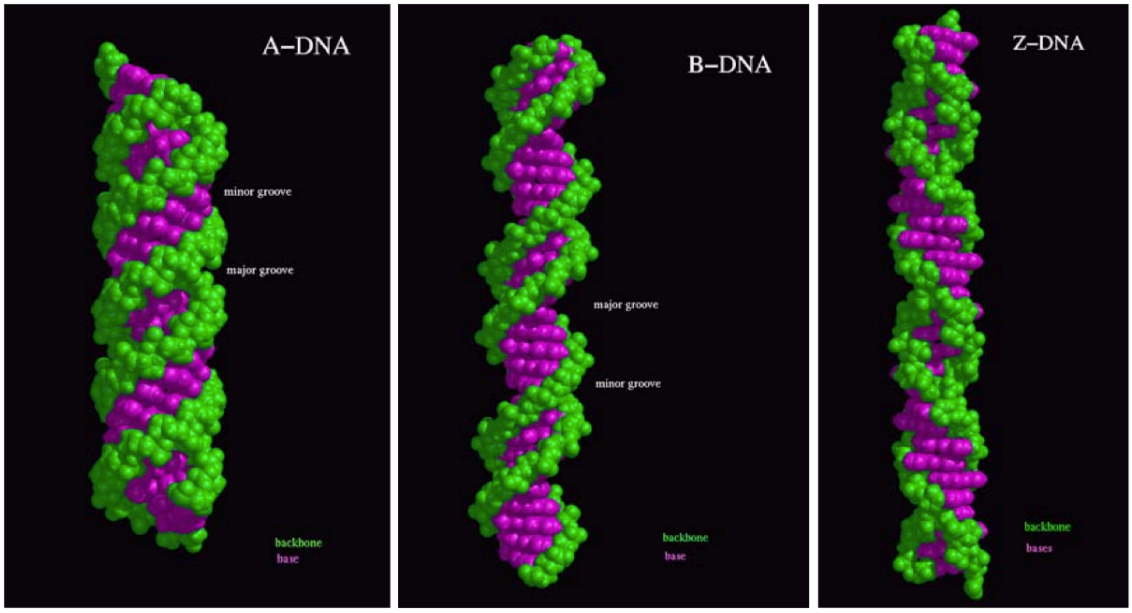

Figure 3: Models of A-, B- and Z-DNA which are the main families of DNA conformations. The backbone is illustrated with green colour while the bases are violet [17].

Hybridisation refers to the annealing of two complementary single strands of a nucleic acid, also called as sticky ends, to form a duplex. Melting temperature (T_m) is used to measure the strength of the duplex. Since the G-C pair is stronger, the duplexes with higher G-C content have higher melting temperature. Also, temperature affects the rate of association of ssDNA into a duplex, and at low temperatures the rate can be estimated using formula (1).

$$k = Ze^{-E_a/RT}, \tag{1}$$

where k is the re-association rate constant, E_a the activation free energy, R the gas constant and T the absolute temperature. The rate is determined in free energy between the unassociated and the transition state [8, p. 178–180]. In figure 4 two duplex molecules with a single stranded overhang are shown. Since the overhangs are complementary to each other they can cohere when mixed in a solution [10]. At higher temperatures, the stability of the double helix is reduced and eventually it becomes unstable and the hybrid melts. Cations help to stabilise the duplex. Hence, the melting temperature decreases at lower salt concentration. Divalent

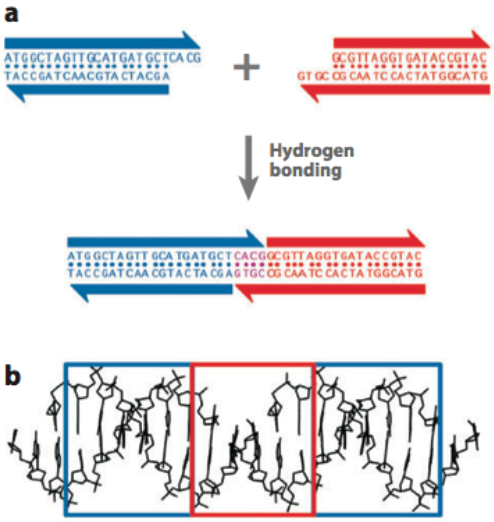

Figure 4: Sticky-ended cohesion. a) The complementary overhangs, called sticky ends, hybridise to form a duplex. b) The interface of two duplex molecules held together by sticky ends can be seen as gaps in the red box [10].

cations, such as magnesium, are more effective in stabilisation of a duplex. Also the duplex length affects the melting temperature, but only when the length is shorter than a few hundred base pairs. These four factors affecting the melting temperature can be combined into an empirical equation that gives the melting temperature for a hybrid DNA [8, p. 178–180].

$$T_m[^\circ\mathrm{C}] = 69.3 + 0.41(\%GC) + 18.5log_{10}M - 500L^{-1} \quad (2)$$

In formula (2) T_m is the melting temperature in celsius, $(\%GC)$ is the percentage of the G-C base pairs, M is the monovalent cation concentration in moles per litre and L is the length of the double helix in number of base pairs [8, p. 178–180]. Web-based algorithms are also available for calculating T_m (for example [18] and [19]). The optimal temperature for hybridisation is normally from 10 to 20 °C below the melting temperature [8, p. 178–180].

2.2 Biocompatibility of DNA

The physiological response to DNA in human body is relevant for example to blood-borne DNA-based nanodevices. The concentration of free DNA in human blood serum is normally very low, 5–40 ng/ml. In normally controlled apoptosis, cells degrade their DNA before releasing it, preventing inflammatory responses. The concentration can increase due to some diseases, such as cancer. Liver is the primary uptake site for free DNA and the uptake speed is higher for ssDNA compared to dsDNA [20, p. 81–83].

In its natural helical state, DNA is normally nonimmunogenic in animals. In human, natural nuclease enzymes, such as plasma nucleases, can rapidly degrade ordi-

nary double-stranded DNA, RNA, synthetic polyribonucleotides, antisense oligonucleotides and various oligodeoxynucleotides placed in human blood serum. Serum factors depolymerise and opsonise post-apoptotic nuclear DNA. Immunoglobulin G (IgG) found in human blood serum and milk can hydrolyse DNA and RNA molecules. Compared to double-stranded oligonucleotides, single-stranded oligonucleotides are more susceptible to hydrolysis. Endonucleases rapidly cut ssDNA with high molecular weight to 20–30 kD fragments [20, p. 81–83].

Solid-phase binding of DNA segments significantly decreases DNA antigenicity due to hindered antibody and nuclease interactions. The risk of insertional mutagenesis from nucleic acid medicines is exceedingly reduced in DNA-based nanodevices as long as they remain intact. Chemical modifications can improve the resistance of oligonucleotides to nuclease attack. Obviously, each modification has to be tested separately since some alterations may cause the synthetic material to become toxic *in vivo*. Moreover, biological activity, such as translational or enzymatic activity, of artificial DNA sequence forming these nanodevices should be investigated in every case [20, p. 81–83].

In some applications, such as controlled drug delivery, efficient cellular uptake should also be considered. Particle size and shape are known to significantly affect the "fate" of delivery vehicles in physiological environment. Since these features are easily controllable, DNA origami nanocarriers can be optimised for specific diseases. DNA itself is polar and its transfection into cells is challenging. Assembling DNA into three-dimensional conformation promotes cellular uptake [5]. Additionally, it has recently been proved that coating of DNA origami structures with virus capsid proteins improves the delivery of origamis into the cells significantly compared to bare DNA origamis [21]. Lipids are a large and important group of biomolecules involved in biological membranes and compartmentalisation, and thus affecting transportation in cells and other organisms. Recent studies have introduced the possibility to construct hybrid systems of DNA nanostructures and lipids. Utilising the exceptional physicochemical features of membrane assemblies makes DNA-based nanodevices even more versatile [22].

3 DNA origamis

Top-down methods, such as different types of lithography, are traditionally used to produce nanoscale objects and structures. These methods usually include removing, subtracting or subdividing bulk material [9]. DNA origami offers a bottom-up method with better precision overcoming the resolution limit of top-down methods [6]. Before discovering the DNA origami method, the self-assembly of DNA-based structures required systematic design of large number of short complementary oligonucleotides. These components have to be combined in perfect equimolar stoichiometry in order to achieve high yield, and the method often requires additional purification steps. Using these older DNA self-assembly methods the complexity of the structures is limited since only basic geometric shapes can be created [1]. DNA origami method offers possibilities to create non-periodical arbitrary shapes with controlled size and nanometer scale resolution. Control over spatial positioning and compartmentalisation make DNA origamis ideal for functionalisation and modifications. DNA origamis can also be produced using method which does not require scaffold strand [4, 23, 24], but in this thesis only scaffolded DNA origamis are discussed.

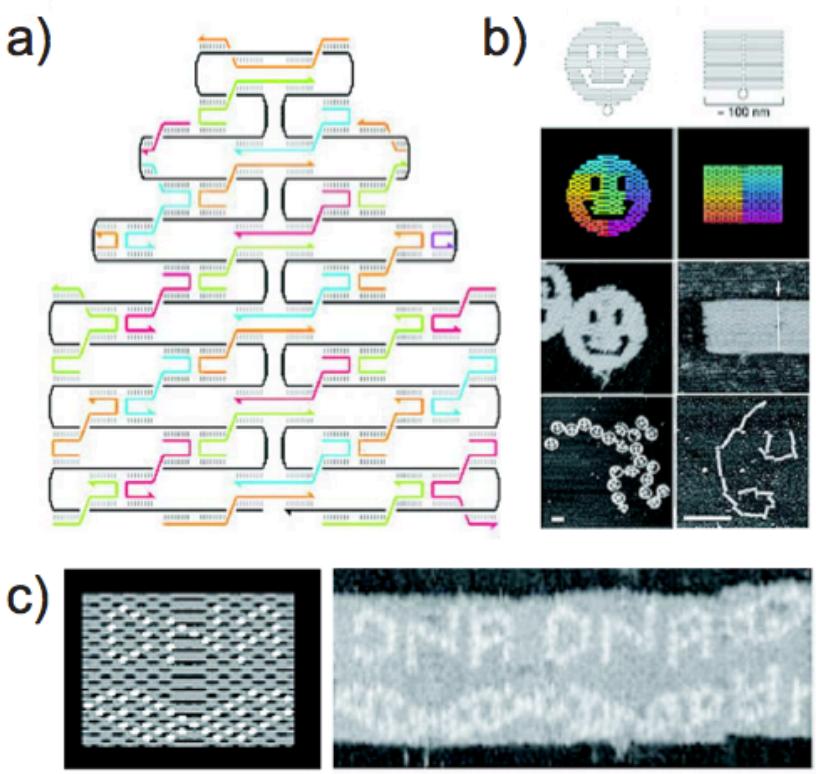

Figure 5: a) The black scaffold strand is folded by orange, green, blue and red staple strands into desired shape. b) Two examples of 2D DNA origamis, a smiley face and a rectangular tile. c) Hairpins can be placed perpendicular to the surface of the origami non-periodically as topological markers with nanometer scale precision [2].

In DNA origami a long single strand of DNA (typically around 7000 nt) serves as a scaffold and it is folded into arbitrary shapes by hundreds of short synthetic oligonucleotides called staple strands (fig. 5). When using the traditional M13mp18 scaffold the length of the scaffold strand determines the size of the 2D structure [25]. However the method can be generalised for any kind of ssDNA molecule [26, 27]. Resulting from the simple but strict rules and energetic favourability of base pairing, the strands are usually binding to each other maximising the number of correctly paired bases and forming a double helical structure. This enables the very precise control over the size and shape of the final nanostructure [28]. DNA origami can also have single stranded domains in addition to double helical domains. Chosen parts of the scaffold strands can be left unpaired or some staple strands can be designed in such a way that a part of them do not bind to the scaffold strand. Unpaired scaffold loops or single stranded overhangs can be used to prevent undesired base stacking interaction at objects' interfaces. An end of a double helix where both strands terminate in a base pair is called a blunt end. Two blunt ends are always compatible which makes the interaction unselective, but on the other hand, the property can be used to strengthen the attachment of two structures. Also, both free staple segments and unpaired scaffold strands can be utilised as hybridisation sites for controlled attachments [29]. Advantages of DNA origami are the experimental simplicity and fidelity of the folding process [28]. DNA-origami structures are known to survive temperatures up to 200 °C [30]. Origami objects can be visualised for example with transmission electron microscope (TEM) or atomic force microscope (AFM).

Figure 6: Square lattice (left) and honeycomb lattice (right) [29].

For multilayered objects DNA helices can be arranged onto a square lattice or a honeycomb lattice. In square lattice each double helix can have four and in honeycomb lattice three neighbors arranged as in figure 6. B-form DNA double helix has helicity of 10.5 bp per full 360° turn. In a honeycomb lattice crossovers can be placed in intervals of 7 bp (fig. 7B), yet so that to the same neighbour the interval is 21 bp. This spacing rule causes local undertwist or overtwist and axial strain. Globally observed, these twists can cancel each other out, or they can be used to create global tunable bending (fig. 7E). In a square lattice system the crossovers can be placed in intervals of 8 bp, the interval between a particular helix pair being 32 bp. This 8 bp interval causes underwinding of every double helix, since the natural helicity of 10.5 bp is adjusted to 10.67 bp per turn. These local twists can cause global twist to the entire object, if not compensated with varying the interval of

the crossovers [29]. Also, close-packed hexagonal lattice and hybrid origami with all three lattice variations in one design have been studied [31].

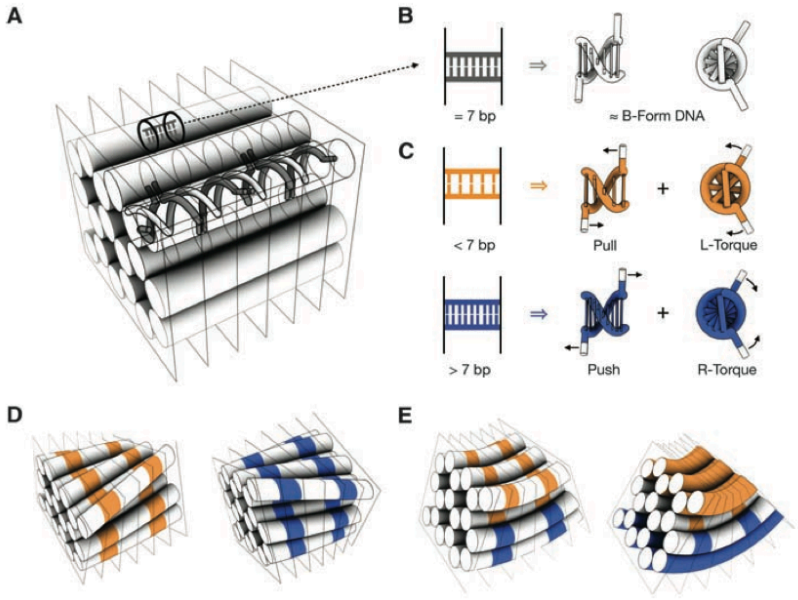

Figure 7: Controlling twist and curvature in DNA bundles. A) DNA double helices are arranged into a honeycomb lattice by crossovers. Rectangular planes mark the locations of staple strand crossovers between neighboring helices. B) Crossovers spaced at 7bp intervals exert no stress on its neighbors and causes no local or global curvature to the structure. C) Crossovers spaced at less than 7bp intervals cause left-handed torque and a pull to its neighbors, while crossovers spaced at more than 7bp intervals cause right-handed torque and a push to its neighbors. D) Site-directed deletions in selected locations (orange stripes) result in global left-handed twisting and insertions (blue stripes) result in global right-handed twisting. E) Selected deletions (orange) and insertions (blue) can also be used to create tunable global bending [32].

3.1 Preparation of DNA origami

The actual building blocks of an origami, the scaffold strand and the staple strands, are mixed with buffer and some salts. Salt requirements differ according to the structure and the complexity of the target object. For example multilayered objects require different salt conditions compared to single layered objects [29]. After mixing, the components are set to a relatively high temperature, where all secondary structures dissolve. Then the mixture is cooled down very slowly, allowing the molecules to find the thermodynamically most favorable conformation and avoid getting trapped in unwanted interactions. This is relatively time-consuming process, since the folding has been found to occur in a very narrow temperature range, at least for simple single-layer structures. However the transition temperature depends on the nature of the design and therefore varies a lot between different origami

structures. If the transition temperature is identified, the process can be speeded up starting slightly above the temperature and finishing slightly below it [33] or by folding at constant temperature [34]. This folding method could play important role when developing methods for mass production of DNA origamis.

Surface patterning can be added onto 2D DNA origami different ways. One example is to use so called hairpins which are placed perpendicular to the surface. These topological markers can be seen as dots in an AFM image. In figure 5b examples of different 2D origami structures are shown and in 5c hairpins are used to create patterning on the surface of an origami [2]. The hairpins are of little use as they are, but they are often used to demonstrate the possibilities for patterning and modifications. For example nanotubes, biotin or fluorophores could be added to origami using the same method.

Although DNA origami structures can be analyzed and imaged without any purification steps, many further treatment procedures and applications require some cleaning steps and removing of the excess of the staple strands. A purification method based on agarose-gel electrophoresis has become widely used. Well-folded structures can be separated from slower migrating products, such as misfolded structures and aggregates, and from faster migrating components, such as the excess staple strands. After the electrophoresis the desired structures can be cut out from the gel and reconstituted into a desired buffer. The method is effective in small scale production if traces of agarose and staining materials are tolerated [35]. Another option for purification is the spin-filtering method. This method requires knowledge about the sizes of different components to be separated allowing the choice of adequate cut-off for the filtering device. This method works best while the molecules' sizes are different enough, at least one order of magnitude. Also, Lin *et al.* have published a method more suitable for bigger scale production based on rate-zonal centrifugation. Molecular species are separated using high centrifugal forces in a density gradient media. It may offer scalable, cost-effective and contamination-free method for purification of larger amounts, such as milligram quantities, of DNA nanostructures [35].

3.2 Preparation of 3D DNA origami

The first successful three dimensional structures were published in 1999 by Nadrian Seeman. Back then, the yield of the final product was low, but the reports proved that 3D structures can be assembled using DNA origami and the methods have significantly improved since [36]. At present, 3D structures can be created at least by two different strategies. Double stranded DNAs (dsDNA) can be bundled together controlling the relative positions of adjacent dsDNAs by crossovers. For instance, tubular and multilayered structures can be formed using this method as illustrated in figure 8. The relative positions between adjacent dsDNAs are controlled by increasing or decreasing the number of base pairs between crossovers. Because of the complexity and high density of the crossovers, folding the DNA strands into target 3D structure using this method has previously required a week-long folding time [25]. Nowadays the time can been narrowed down by determining the right folding

temperature [34]. An other strategy is to fold separate 2D origamis and afterwards to attach these to each others by connecting strands. One variation is illustrated in figure 11 where a box is constructed by connecting six individual rectangular planes using interconnection strands [25]. Like described in the beginning of chapter 3, origamis can polymerise also via blunt ends. This stacking interaction is relatively strong but not programmable or selective [37].

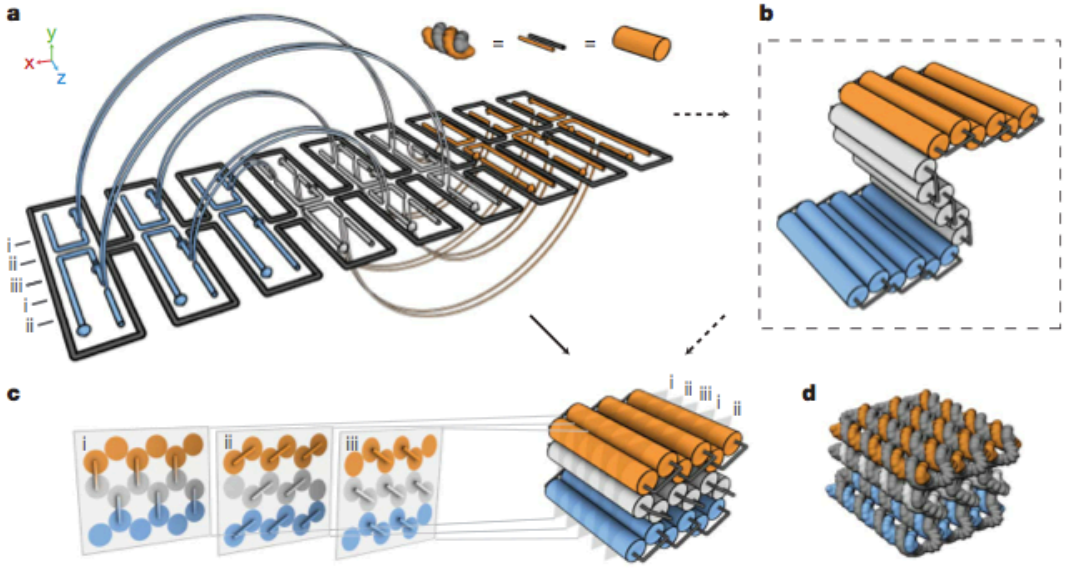

Figure 8: Folding 2D origami into 3D object. a) Dark grey scaffold strand and blue, white and orange staple strands run parallel to the z-axis forming two-dimensional unrolled model of the target shape. b) In the dashed box, in a half-rolled model, cylinders represent double helices while loops of unpaired scaffold strands link the ends of adjacent helices. c) Underneath are cross-sectional slices (i-iii) of the honeycomb arrangement spaced apart at seven base pair intervals, d) and finally, the atomistic model of the target shape [38].

Even though the 7kb M13 genome is currently the primary choice for the source of scaffold, it is unlikely the optimal scaffold sequence for all possible DNA objects. To scale up and create larger DNA origami structures one alternative is to use a longer scaffold (fig. 9, top). This approach using a single long scaffold is traditional and simple, but in order to create large structures it can be inconvenient. To build a gigadalton DNA object, the single scaffold should be over one megabase long which could be mechanically fragile and difficult to synthesise. Another alternative is to fold multiple separate origami objects, preferably using scaffolds with distinct sequences, and link these "super-tiles" together to form larger superstructures like in figure 9 (bottom) [39]. Zhao *et al.* have demonstrated a strategy to scale up further and create "superorigamis". In the method first, a loose framework is created by folding a single stranded DNA scaffold with a collection of bridge strands (fig. 10, top, right). Next, multiple individual DNA origami tiles are directed onto the framework to act as large staples and to create a "superorigami" structure. This

method allows the construction of larger architectures, but still retaining the spatial addressability [40].

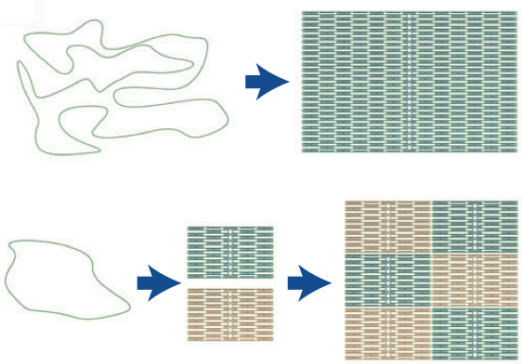

Figure 9: Scaling up the size of a DNA origami. To overcome the dependence of the length of the viral M13 genome a longer scaffold strand can be used (top) or pre-formed structures can be assembled to supramolecular assemblies (bottom) [39].

3.3 Applications

In order to create a proper molecular carrier system for mammalian cellular delivery, a DNA object has to fulfill at least three criteria. First, the structure has to be stable both in the extracellular space and in the cytoplasm long enough to accomplish it's assignment. Second, it can not cause any toxic side effects and third, it has to be tolerated by the mammalian immune system. Numerous studies about DNA stability in physiological environment has been done during the past decade and DNA origami and other DNA constructs have been proved to be highly stable compared to duplex plasmid DNA when exposed to multiple endonucleases. DNA origami structures has also been proved to maintain their structural integrity when exposed to various cell lysates [41].

The genetic basis, hence the therapeutic target, is known for numerous diseases, which makes the design of selective targeting possible. From amongst other potential alternatives for gene transfer, viruses are very effective, but safety concerns limit their usage. Then again, for example cancer is extremely complex and not fully understood, which indicates the need for multifunctional delivery systems for combination therapies. DNA nanotechnology and DNA origami method have been developed to the point where they could offer answers and solutions for gene and drug delivery applications [5]. Schüller *et al.* showed in their study that hollow DNA origami tubes could substitute standard carrier system, Lipofectamine, to deliver cytosine-phosphate-guanine (CpG) sequences into spleen cells to trigger immune system. They proved the DNA origami -based method to be more efficient and nontoxic compared to the standard Lipofectamine system [41]. Also Li *et al.* have delivered CpG oligodeoxynucleotides (ODNs) into macrophage-like RAW264.7 cells using three-dimensional DNA tetrahedra. [42]

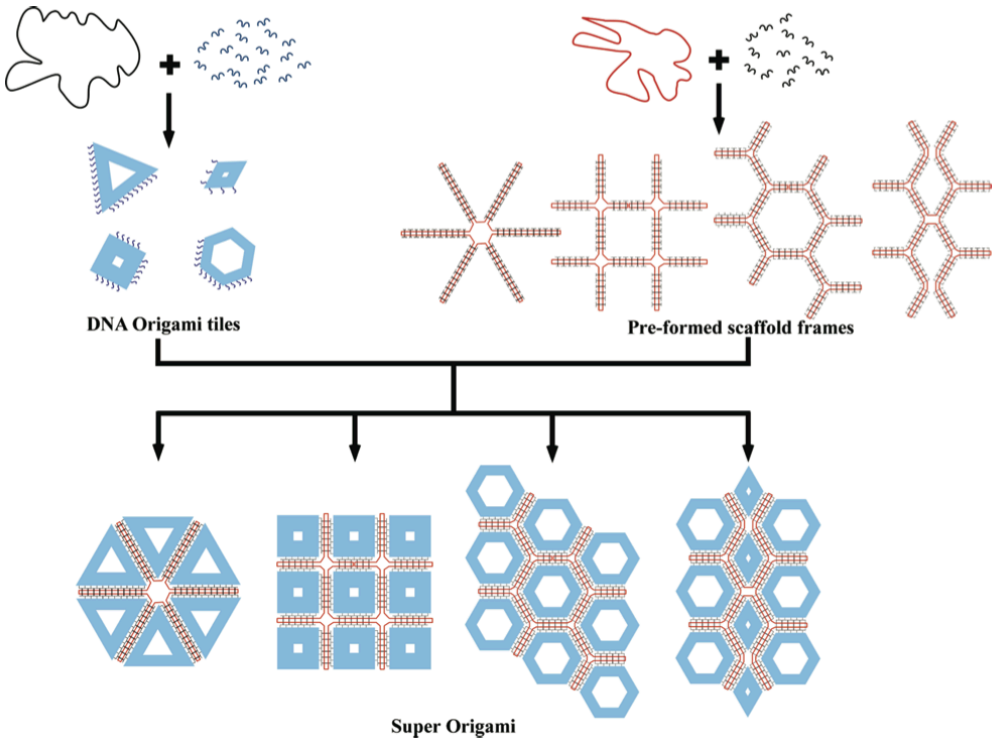

Figure 10: "Superorigami" structures can be formed using prefolded framework and traditional DNA origami tiles. A single stranded DNA scaffold is folded into a loose framework with the help of bridge strands (top, right). Separately folded individual DNA origami tiles (top, left) are then directed onto the framework. The origami tiles act as staples and together with the framework they form a "superorigami" (bottom) [40].

Cargo can be loaded into the nanocarrier device by different ways depending on the size and chemical properties of both the carrier and the cargo. For instance nucleic acids can be directly integrated into the nanostructure of the carrier by design. Antisense, aptamer and CpG sequences have been loaded into wireframe DNA tetrahedra structures using this approach (fig. 12). Second possibility is passive physical entrapment. This is somewhat inefficient, but simple and successful method if the cargo fits inside the carrier and is compatible with the assembling process, such as thermal annealing. This approach has been used to load gold nanoparticles inside wireframe DNA tubes. Also partially hybridised strands, overhangs, can be incorporated on both carrier and cargo with complementary sequences permitting direct attachment [5].

Also various other molecules and particles can be used to functionalise DNA origami. For example ligands, small molecules that bind to DNA double helix, or peptide molecules, can be used to attach particles on a DNA origami object [25]. It has also been proved that DNA origami objects can be either prefabricated for material assembly, or the desired materials can be assembled simultaneously with the origami [43]. Dendrons, repetitively branched molecules, have been attached to DNA

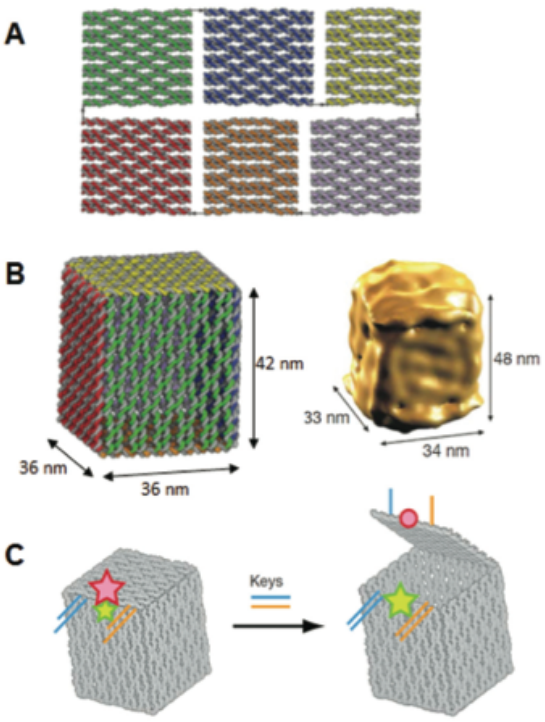

Figure 11: Design and construction of a three dimensional DNA origami box. a) Six independent plates are annealed and then attached with connecting strands. b) The design and a model of the box reconstructed from cryo-EM images. c) The lid of the box is opened with specific and selective DNA strands. The opening event can be monitored by fluorescence resonance energy transfer (FRET) [25].

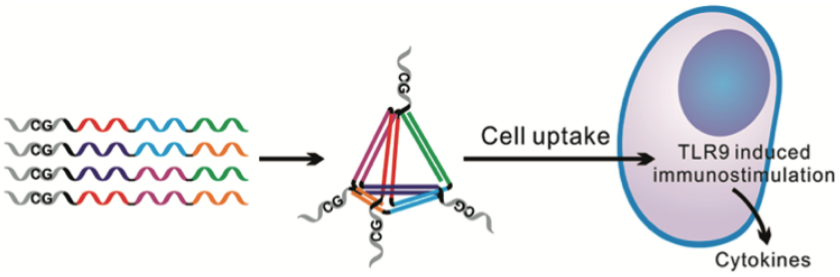

Figure 12: A schematic of the assembly of CpG-bearing DNA tetrahedron. Synthetic CpG oligodeoxynucleotides (ODNs) can bind to endosomal Toll-like receptor 9 (TLR9), induce its conformational changes and activate it, triggering a signaling cascade leading to remarkable immunostimulatory responses [42].

origamis in order to create structures that can be controlled with external stimuli [44]. Silver nanoparticles have been assembled on DNA origami tiles to create bow-tie antenna configurations [45]. Biotin-avidin interaction is widely used in biological sciences. Avidin protein is found in raw egg white and it can strongly bind up to four

biotin molecules. Because of the small size of the biotin molecule (244.31 g/mol), it rarely affects other molecule's properties. For example carbon nanotubes have been attached onto DNA origami template using biotin-avidin interaction [30]. In this thesis biotin-avidin interaction is used to attach two different enzymes inside hexagonal nanotubes.

2D DNA origami platforms can be used to study chemical processes since the method allows direct monitoring of chemical reactions on the single-molecule level. Even the preparation of macromolecules in a highly selective manner is possible [1]. DNA origamis has also been used as helpers to determine protein structures with NMR [46, 47], solid-state nanopore gatekeepers [48, 49], chiral plasmonic nanostructures with tailored optical properties [50] and to study transporting motor proteins in vitro [51]. DNA self-assembly can be utilised to integrate different physicochemical processes and various components within one system. For example, multiple enzymes could be arranged inside origami-based reaction chambers, while their reactions could be coupled to photo-induced electron transfer or energy transfer processes, which could proceed along DNA-based antenna systems and electron transport chains [52].

One noteworthy detail is the influence of compartmentalisation, spatial organisation, geometry and proximity to reaction kinetics. Two compounds in close proximity can react with each other with a higher rate compared to same compounds locating further from each other. This plays an important role especially in reactions with high activation barriers or compounds with low concentration [52]. This is normally the case in cellular environment where many synthetic pathways in cells involve multiple enzymatically catalyzed steps, but at the same time require high yield and specificity [53]. Since each individual position on a 2D structure has its own unique sequence information, DNA origami offers a platform for arranging reactants with nanometer scale, adding multiple compounds to specific order and even controlling the orientation of the molecules. If a reaction includes several steps, the stability, toxicity and diffusion of the intermediate compounds has to be considered. With appropriate arrangement and spatial organisation possible side-reactions can be prevented and the desired reaction flux can be improved. The effect of spatial arrangement depends on the physical process considered. In figure 13 three different ways to arrange compounds in relation to DNA origami are shown [52].

A method called dielectrophoretic trapping has also been developed to trap DNA origami objects between nanoelectrodes, which allows controlled positioning of objects on a chip. This opens new possibilities to combine bottom-up and top-down fabrication methods and to utilise DNA origami objects in the field of nanoelectronics [54]. On the other hand, conductivity and conductance mechanisms of DNA are still not fully understood and these questions have to be answered in order to make use of DNA origami in electronics applications [15].

Recently, various kinds of functional nanoscale robots and devices have been developed based on DNA origami structures. Kuzuya *et al.* published a three-state nanomechanical device which can switch between three different conformations in a controlled way [55]. Torelli *et al.* have designed and produced a prototype for a DNA origami nanorobot which is able to respond to an external stimulus and

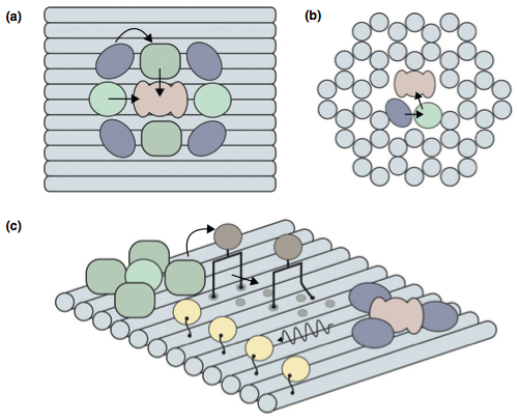

Figure 13: a) Components of complex pathways can be arranged into close proximity on DNA origami in order to improve the control over reaction fluxes and to reduce side reactions. b) Diffusive loss can be reduced by encapsulation of the components into artificial reaction chambers. Also, c) molecular walkers can be used to transport components between two reaction centers to prevent diffusive loss [52].

to deliver a cellular compatible message based on the stimulus. Also, Douglas *et al.* introduced an autonomous DNA nanorobot, which can sense inputs from cell surface and reconfigure its own structure for cargo delivery [56]. In figure 11 the "lid" can be opened with a specific DNA sequence acting as "keys" and the possible cargo can be released in a controlled way [25]. These kinds of functional robots have great potential for *in vivo* biosensing applications and controlled delivery of biological activators [57].

4 Enzyme nanoreactors

Compartmentalisation is one of the techniques that cells use to achieve a high level control over chemical processes, for instance, the order in which enzymes react. The compartmentalisation can also protect the cell from its degrading contents, as is the case with lysosomes. Compartments can furthermore serve as scaffolds for the precise positional assembly of enzymes that work together in cascade reactions [58]. Controlled spatial arrangement can increase the efficiency of multistep processes, allow feedback mechanisms and enable the use of unstable intermediates. For instance in mitochondria enzymes involved in the citric acid cycle are positioned on a surface, interior or membrane of a compartment, or any combination of these. Compartmentalisation and positional arrangement together allow a cell to perform multiple different chemical processes simultaneously without them affecting each other in an uncontrolled way [59]. The communication and transportation between different compartments in a cell can occur via an active pathway with the help of membrane protein channels, or via a passive pathway utilising diffusion [60]. Recently Fu *et al.* have studied DNA based multi-enzyme complexes which utilise an artificial swinging arm as a transfering medium [61].

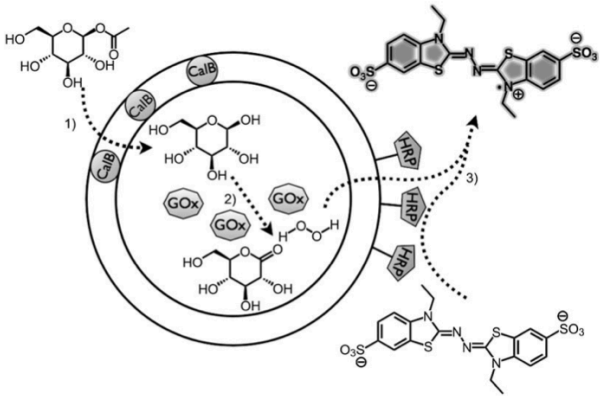

Figure 14: A schematic representation of a three-enzyme cascade reaction. *Candida antarctica* lipase B (CalB) is embedded in the polymersome membrane, glucose oxidase (GOx) is in the inner aqueous compartment and horseradish peroxidase (HRP) is positioned on the outer surface of the polymersome. In the nanoreactor glucose acetate is converted to glucose by CalB and futher oxidised to gluconolactone by GOx. At the same time hydrogen peroxide is produce and it is used by HRP to oxidise 2,2'-azinobis(3-ethylbenzothiazoline-6-sulfonic acid) (ABTS) to $ABTS^+$ [58].

Polymersomes are spherical aggregates with a bilayer architecture formed by the self-assembly of amphiphilic block copolymers. The properties of a polymersome are tunable by the block copolymer synthesis, but the downside is the low permeability

to aqueous solutions, which restricts their usage as nanoreactors [58]. However, recent developments in polymer technology have enabled the control over membrane permeability of polymeric nanoreactors. Polymersomes have been studied as enzymatic reactors using only one enzyme or two different enzymes entrapped in two separate polymersomes [59]. Van Dongen *et al.* have studied a three-enzyme cascade system where the enzymes are positioned on three different parts of a polymersome, the membrane, the interior and the outer surface (fig. 14) [58]. The enzyme activity have even been shown to decrease slower over time when encapsulated inside a polymersome, compared to free enzymes [60].

The natural purpose of most viruses is to store and transport viral RNAs or DNAs. Hence, after removal of the genome, the capsids of viruses provide a uniquely defined inside environment to entrap inorganic nanoparticles, polymers and enzymes [62]. Up to date, besides viruses [62, 63, 64] and polymersomes [58, 65], various materials and methods have been used to encapsulate enzymes, including carbon nanotubes [66, 67], sol-gels [68], inorganic nanocrystal-protein complexes [69] and nanosized ferrous matrices [70].

5 Materials and methods

The aim of this work was to attach three glucose oxidase (GOx) or horseradish peroxidase (HRP) enzyme molecules (fig. 15) inside an origami tube and to attach two of these tubes containing different enzymes to each other. We use the strongest known non-covalent interaction, biotin-avidin link, as the attachment method for the enzymes and the hybridisation of overhangs for the DNA origami tubes. The used chemical reactions catalyted by HRP and GOx are illustrated in figure 16. The basic idea of the nanoreactor is shown in figure 17. The DNA origami monomer unit is approximately 30 nm long hollow hexagonal tube with a wall thickness of 6-7 nm. More precise dimensions are shown in figure 17A. The hypothesis is that the reaction rate of the chosen catalyted reaction series increases if the enzymes are situated inside two origami tubes attached to each others compared to the situation where the origamis are separately in a solution. In some cases, especially in low concentrations, the reaction rate for this kind of nanoreactor system could even be higher than for free enzymes without any origamis.

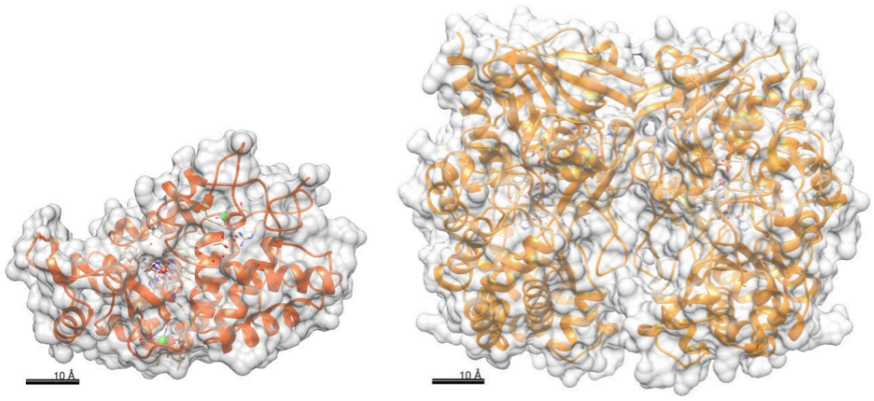

Figure 15: Models of horseradish peroxidase (left) and glucose oxidase dimer (right). The length of the scale bars is 10 ångström or 1 nm. Adapted from [71].

HRP-GOx enzyme pair has been previously used in the context of DNA origami at least by Müller *et al.* [72], Fu *et al.* [73] and Fu *et al.* [53]. In these previous studies the enzymes have been attached either on a plane, on an outer surface of other structures or inside a single origami tube. In this thesis project the goal is to attach the enzymes inside two separate origami tubes and utilise the benefits of compartmentalisation. The individual tubes can be produced and functionalised separately allowing, for instance, the use of molecules with different attachment methods. In this thesis two tubes are combined, but the system could be extended with additional tubes.

5.1 Preparing DNA origami

DNA origami tubes were designed using caDNAno software [74]. caDNAno is an open-source graphical-interface-based computer-aided-design environment and

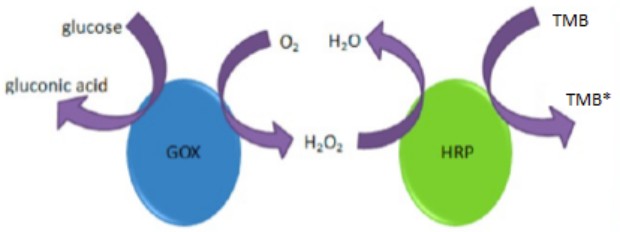

Figure 16: Schematic of the reactions of the Glucose oxidase/Horseradish peroxidase (GOx/HRP) enzyme cascade. GOx enzyme (blue) turns glucose to gluconolactone. At the same time hydrogen peroxide (H_2O_2) is formed from water (H_2O) and oxygen (O_2). HRP enzyme (green) uses the H_2O_2 to oxidise tetramethylbenzidine (TMB) to TMB diimine (TMB*). Adapted from [73].

it is available on www.cadnano.org. Honeycomb lattice was utilised and the designs are shown in appendix A. The stability and possible fluctuations of the designed structure were tested submitting the caDNAno file to CanDo webpage (`http://cando-dna-origami.org/`) [29]. M13mp18 bacteriophage containing 7249 nucleotides was used as the long scaffold strand and it was purchased from New England Biolabs. The staple strands were purchased unpurified in RNAse free water from Integrated DNA Technologies (IDT) at 100 nM concentration.

The designed structure was first tested without modified strands to ensure the origami folds correctly. The scaffold strands and the staple strands were mixed with TAE buffer (Invitrogen by life technologies™, UltraPure™ 10 x TAE buffer: 400 mM tris(hydroxymethyl)aminomethane (TRIS) acetate and 10 mM ethylenediaminetetraacetic acid (EDTA)) magnesium and sodium chloride (NaCl). Volumes, chemicals and concentrations are shown in table 1. The staple strands were added in 10-fold excess concentration. The solution was annealed in a thermal cycler (Finnzymes Instruments Piko Thermal Cycler). A pre-programmed method was used in which the solution is first heated up to 65 °C and then slowly cooled down. From 65 °C to 60 °C the temperature is decreased at 1 °C/15 min. After that the temperature is dropped from 59 °C to 40 °C at 0.5 °C/90 min.

Table 1: Components of the folding solution.

Volume (µl)	Material	Concentration	Final concentration
10	M13mp18 scaffold strand	100 nM	20 nM
20	Staple strands	500 nM	200 nM
5	TAE buffer	10 x	1 x
5	Sodium chloride, NaCl	50 mM	5 mM
10	Magnesium, Mg^{2+}	110 mM	22 mM

After folding, excess of the staple strands were removed by spin filtration using 100 kDa Amicon filters and a Sigma centrifuge (model 3k30). 50 µl of sample and

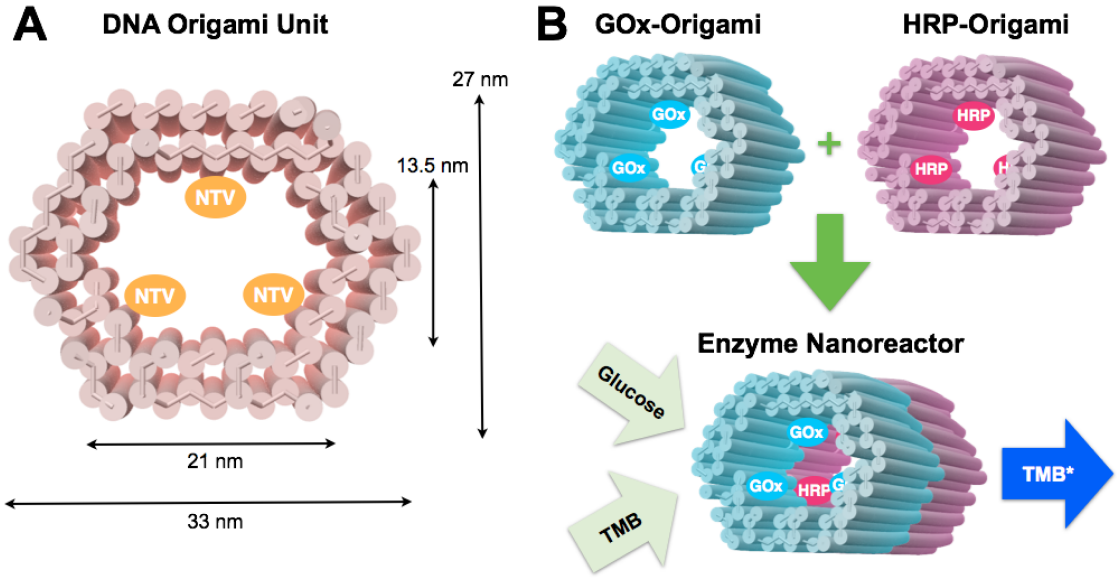

Figure 17: A) CanDo-simulated shape and dimensions of a basic DNA origami unit used as a building block of a nanoreactor. The length of an origami is about 30 nm. NTVs indicate neutravidins, which are anchored to the inner surface of a tubular origami via biotinylated strands protruding from the origami. NTV acts as a binding site for biotinylated enzymes. B) A schematic working principle of the nanoreactor. Two separately fabricated origami units are equipped by biotinylated glucose oxidase (GOx) or horseradish peroxidase (HRP) via biotin-avidin interaction. The units are linked together via base-pairing resulting in a nanoreactor that is able to perform an enzyme cascade reaction: 1) Glucose enters the nanoreactor and in the presence of oxygen a hydrogen peroxide (H_2O_2) is released at the GOx enzyme site. 2) 3,3',5,5'-tetramethylbenzidine (TMB) is oxidised at the HRP enzyme as the diffused H_2O_2 is reduced to water. The formation of TMB diimine (TMB*) is detected by spectrophotometer (absorbance at the 650 nm) [75].

450 µl buffer (1 x TAE, containing 20 mM Mg^{2+}) were pipetted into the filter. The samples were centrifuged for two rounds at 14 000 rcf (relative centrifugal force) at 20 °C (each round for three minutes). Between each round, the flowthrough was removed and 450 µl of fresh buffer was added. For the third round the duration was increased to five minutes keeping the other parameters the same. Finally, to recover the DNA origami sample, the filter was turned upside down and placed into a new Eppendorf tube and centrifuged for two minutes at 1000 rcf. After the filtration, the concentration of the origami was estimated to be around 20 nM.

Also the attaching of two tubes was first tested without the enzymes. Two monomer origamis were connected together by hybridisation of 32 short (3-6 bases) sequences. The short sequences sticking out at the end of one unit were paired with free scaffold sites located at the edge of another unit (fig. 18). Also blunt ends were used to strenghten the interaction between two origami tubes. In order to prevent

the formation of multimers, the other end of the origami unit was passivated by overhanging single-stranded poly-T sequences (TTTTTTTT). 80 poly-T overhangs were used for GOx-origami and 77 for HRP-origami. The monomer units were folded separately and then attached into dimers within 1-day incubation at room temperature. By choosing the strands that connect the units uniquely, this method could be generalised for well-defined modular multimers.

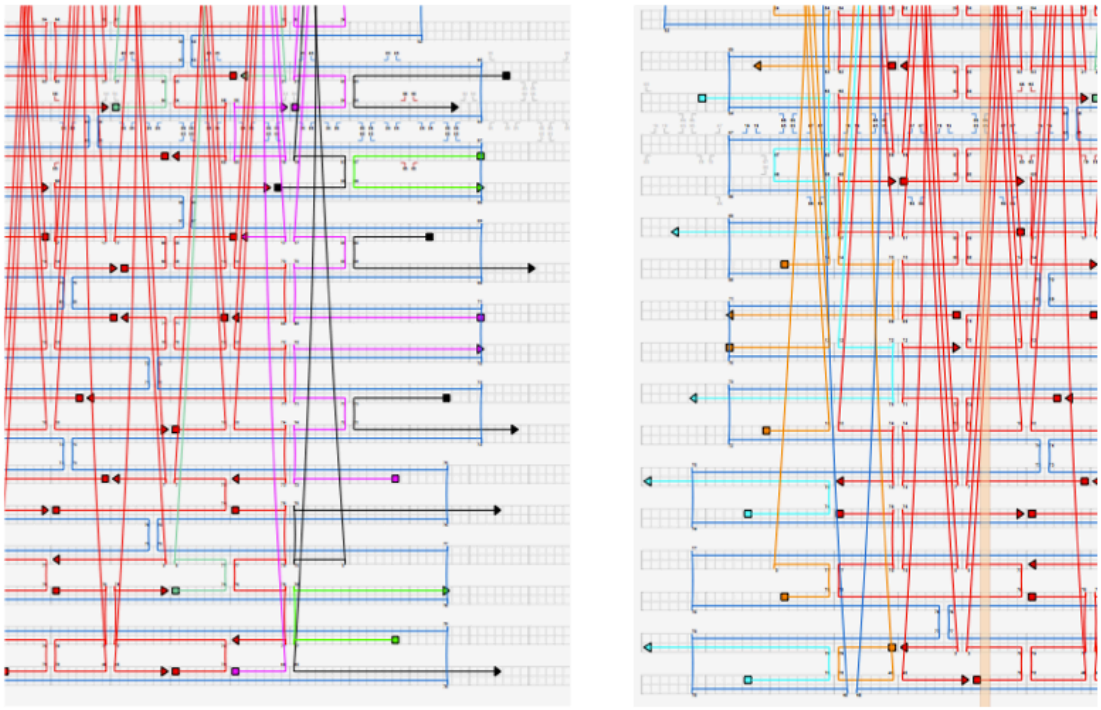

Figure 18: Screenshots from caDNAno software demonstrating the attachment method. The black and turqoise staple strands sticking out at the ends of the tubes hybridise with the unpaired bases of the scaffold strand in the other origami structure [74].

5.2 Analysing the DNA origami

The folded origamis were analysed with agarose gel electrophoresis. Agarose gel forms a 3D network with pores whose size depends on the concentration of the agarose in the matrix. In the method an electric field is ran through the chamber making the sample molecules move along the gel with speed depending on the size, shape and charge of the molecule [8]. The gel was prepared mixing agarose, buffer and magnesium. Ethidium bromide was used as a fluorescent tag since the intensity of its orange colour will increase almost 20 times after binding to DNA.

Because the aim was to see if the folding of the origami was successful, a reference sample was prepared using the same recipe as in table 1 but replacing the staple strands with the same volume of purified water. BIO-RAD Power Pac Basic equipment and 1–2 % agarose gel were used. 15 µl of each sample were stained with

3 µl loading dye (6x Gel Loading Dye Blue, New England Biolabs) and then 15 µl of this solution was pipetted to the wells of the agarose gel. The chamber was filled up with a buffer solution (1 x TAE + 11 mM Mg^{2+}) and the voltage was set to 90 V. Afterwards the gel was imaged using ultraviolet light (BIO-RAD Gel Doc^{TM} EZ Imager) (fig. 19).

DNA origami concentrations for all samples were estimated using Beer-Lambert relation as shown in formula (3), where A_{260} is the absorbance at 260 nm wavelength, ϵ_{260} is the approximated extinction coefficient (0.9 * 10^8 M^{-1} cm^{-1}) [76] and l is the length of the light path in centimeters. The concentrations were determined using BioTek Eon microplate spectrophotometer or Perkin-Elmer Lambda 950 UV/Vis Spectrometer.

$$A_{260} = \epsilon_{260} c_{DNA} l \tag{3}$$

The origamis were also imaged using Fei Tecnai 12 Bio Twin transmission electron microscope (TEM). Formvar carbon coated or carbon only copper grids (Electron Microscopy Sciences) were used and they were cleaned using oxygen plasma treatment (Gatan, Model 950 Advanced Plasma System). 3 µl of sample were placed to the grid and excess of the solution was blotted. Then the sample was treated with 3 µl of aquous 0.5 % uranyl acetate solution twice in order to stain the sample.

5.3 Functionalising the DNA origami

To functionalise the origamis three staple strands were replaced with strands with an additional biotin molecule attached to the 5' end of the strand. The precise places of the modifications in the designs are shown in appendix A. Assuming that only one of each enzymes are attahed to the nanoreactor, the theoretical distances between GOx and HRP enzymes are 25, 27, 28, 30, 31, 33 and 35 nm. The biotinylated strands were added to the folding solution like any other staple strand and the excess amount of strands were removed after folding like described previously.

Next, neutravidin (Thermo Scientific, 1 mg/ml in PBS) was added in 200-fold excess concentration compared to biotinylated staple strands and incubated overnight at room temperature shielded from light. Reference samples were prepared similarly, but replacing the neutravidin with the same volume of water. The solutions were then spin-filtered as described above using 1 x TAE buffer including 20 mM Mg^{2+}.

Biotinylated horseradish peroxidase was added in 20-fold excess to origamis including neutravidin. Solutions were incubated over night in room temperature. After incubation the samples were spin-filtered as before using 1 x TAE (including 20 mM Mg^{2+}) as a buffer. Biotinylated glucose oxidase (purchased from VWR/Rockland Inc.) was added in 200-fold excess to origamis the same way as HRP. The excess of GOx was not spin-filtered due to its challenging size (M_w(GOx)=160 000 g/mol). The enzyme is too large for previously used Amicon filters with 100K cut-off. Also Pall Nanosep centrifugal device with 300K cut-off was tested, but the origamis appeared to fall through the filter because of too big pore size.

The activity of the enzymes attached to the origamis were quantitatively measured utilising spectrophotometer (BioTek Eon microplate spectrophotometer or

Perkin-Elmer Lambda 950 UV/Vis Spectrometer). The enzyme activities were first measured separately having only one of the enzymes attached inside the origami tubes. This was to simultaneously prove the successful selective attachment of the enzymes. To simplify the analysis, other reactants were added in excess amounts. For HRP-origami measurements TMB-H_2O_2 substrate was prepared. The ingredients and amounts are listed in table 2. For GOx-origami TMB-glucose substrate was prepared and the amounts are shown similarly in table 3.

Table 2: Tetramethylbenzidine hydrogen peroxide substrate.

Volume	**Material**
1 ml	TMB (0.2 mg/ml in DMSO)
9 ml	Sodium acetate (0.005 M, pH 5)
4 µl	Hydrogen peroxide

Table 3: Tetramethylbenzidine glucose substrate.

Volume	**Material**
300 µl	TMB (0.2 mg/ml in DMSO)
1200 µl	Sodium acetate (0.005 M, pH 5)
200 µl	glucose (0.1 M)

6 Results

The folding of the origami was analysed with agarose gel electrophoresis and the results are shown in figure 19.

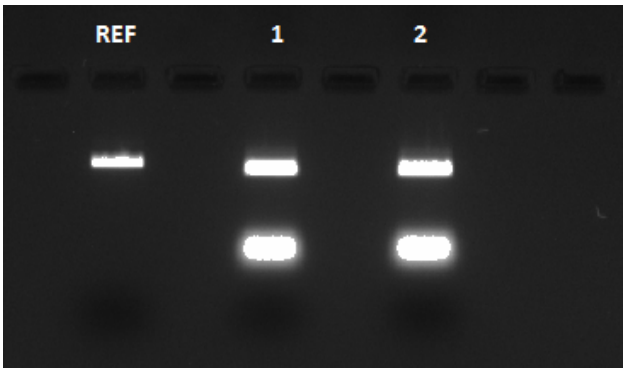

Figure 19: Gel electrophoresis figure of scaffold strand as a reference (REF) and two identical samples (1 & 2) from different folding tubes.

In figure 19, on the left is a sample of M13mp18 scaffold strand in the same concentration and conditions as the origamis on the right. The origamis are not centrifuged, as in the leftover staple strands are still in the solution and they produce the bright strands below the two origami samples on the right. For TEM imaging Fei Tecnai 12 Bio Twin transmission electron microscope was used and the pictures are shown in figure 20A. More TEM images are shown in appendix B. Based on the TEM figures of the monomer origamis, a conclusion was made that the yield of the origamis was quite high and the folding procedure was successful. Also, the attachment of two monomer origamis into a dimer was also successful (fig. 20B and 20C) and the yield was approximated to be close to 90 % (Calculated from TEM images, see figures in appendix B). In figure 20 also the gel electrophoresis results are shown of both monomer and dimer structures, which confirms the successfull dimerisation with high yield. The close-up images in the middle of the figure 20 correspond well with the CanDo simulation of the design.

The activity measurement results for HRP-origami are shown in figure 21A. For all activity measurements the substrates were added in excess amounts and the product concentration, stating the colour change of TMB, was detected at wavelength of 650 nm using BioTek Eon microplate spectrophotometer and Take3 micro-volume plate. The plain substrate was used as blank reference. The reference sample contains the same amount of similarly prepared origami except the avidin is replaced with the same amount of water. Since the biotinylated enzyme has no attachment site the measurements also proves the effectivity of the spin-filtering purification. The HRP-origami shows higher activity compared to the reference sample. The initial concentration of HRP-origami was estimated to be 3 nM and it was mixed with TMB-H_2O_2 substrate in 1:99 ratio. 2 µl of this solution and references were used for measurements. Since the concentrations are in nanometer scale and volumes in microliter scale, the measurements are rough approximations and too exact

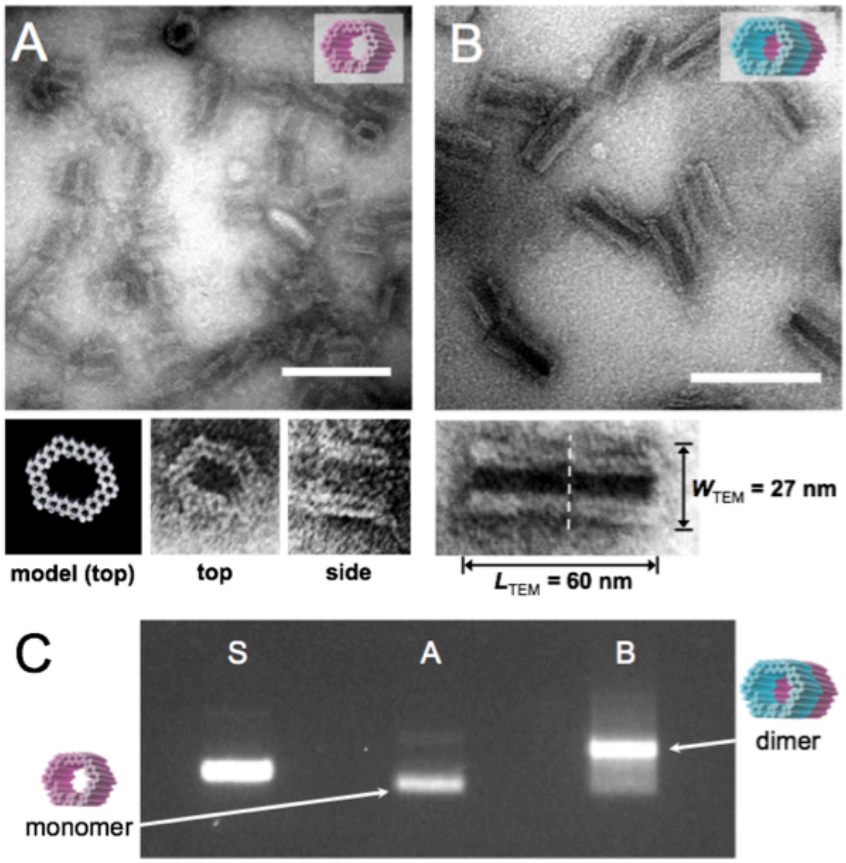

Figure 20: A) TEM micrographs of single DNA origami units. Close-up images of two orthogonal orientations of the DNA origami unit correspond well with the CanDo-prediction of the structure. B) TEM micrograph of dimer nanoreactors. The dashed line in the close-up image indicates the interface of two units. Roughly 86 % of the units formed correct dimers during the assembly (calculated from the TEM images, see appendix B). Scale bars in A and B are 100 nm. C) Agarose gel electrophoresis: S indicates M13mp18 scaffold reference, A contains single origami units (monomers) and B is two units attached to each other (dimers), similarly as in subfigures A and B. Monomers are decently folded (lane A) and the intense additional band in lane B indicates a successful formation of dimers [75].

quantitative comparisons between different samples should be avoided. This can also explain the differing starting points of samples and references in all curves in figures 21 and 22.

The activity results for GOx-origami are shown in figure 21B, in which the blank values are already subtracted from both curves. 20 µl of sample and 10 µl of HRP enzyme (0.0022 mg/ml) were added to 1.7 ml of TMB-glucose substrate The reference origami is prepared exactly the same way as the sample origami except the avidin is replaced with the same amount of water. The GOx-origami shows significantly higher activity compared to the reference origami. The measurements are done using Perkin-Elmer Lambda 950 UV/Vis Spectrometer and standard plastic cuvettes.

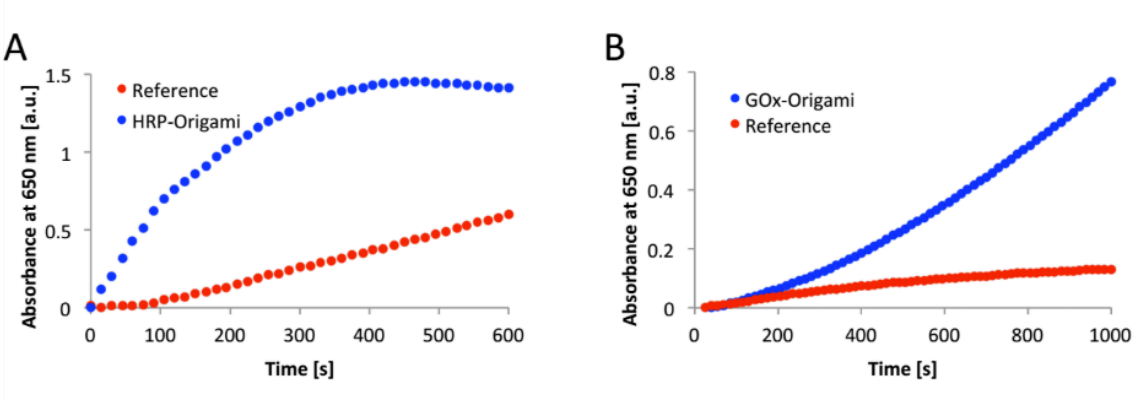

Figure 21: Change in TMB* absorbance as a function of time in arbitrary units. In both graphs the plain substrate is used as a blank and the values have already been subtracted from the curves. A) Progress curve for DNA origami equipped with HRP (blue). The reference (red) is same amount of DNA origami fabricated and treated similarly but without the neutravidin modifications. The TMB-H_2O_2 substrate is added in excess amount and the absorbance is measured with a spectrophotometer at wavelength of 650 nm. B) Progress curve for DNA origami equipped with GOx (blue). The reference (red) is same amount of DNA origami fabricated and treated similarly but without the neutravidin modifications. The TMB-glucose substrate and the b-HRP enzyme are added in excess amounts and the absorbance is measured with a spectrophotometer at wavelength of 650 nm [75].

For both monomer origami samples the results indicate successfull binding for the enzymes to the origami and also, the effectiveness of spin-filtering as a purification method for removing the excess amount of enzymes.

The progress curves for dimer origami sample and reference are shown in figure 22. The measurements are done using BioTek Eon microplate spectrophotometer and sterile 96-well Tissue Culture Plates from VWR. The initial concentration of dimer origami was estimated to be 0.1–1 nM. 40 µl of dimer origami and reference origami was mixed with TMB-glucose substrate so that the final volume for measurements was 300 µl. The reference dimer is similarly prepared dimer origami without the avidin binding sites and the blank smaple is plain substrate. The dimer origami sample shows significantly higher product concentration compared reference. Like in monomer unit measurements the substrate is added in excess amount so that the production and diffusion of intermediate product H_2O_2 is the constraining phase. For all the activity measurements the origami samples show significantly higher activity compared to reference samples. This proves also the absence of unspecific binding of enzymes to origami.

In figure 23 the initial rate of reactions for the single monomer origami units and the dimer nanoreactor are compared to the reference samples. Both monomer units and dimer nanoreactor clearly outdo the activity of the reference samples. The difference is even more pronounced in the case of the dimer.

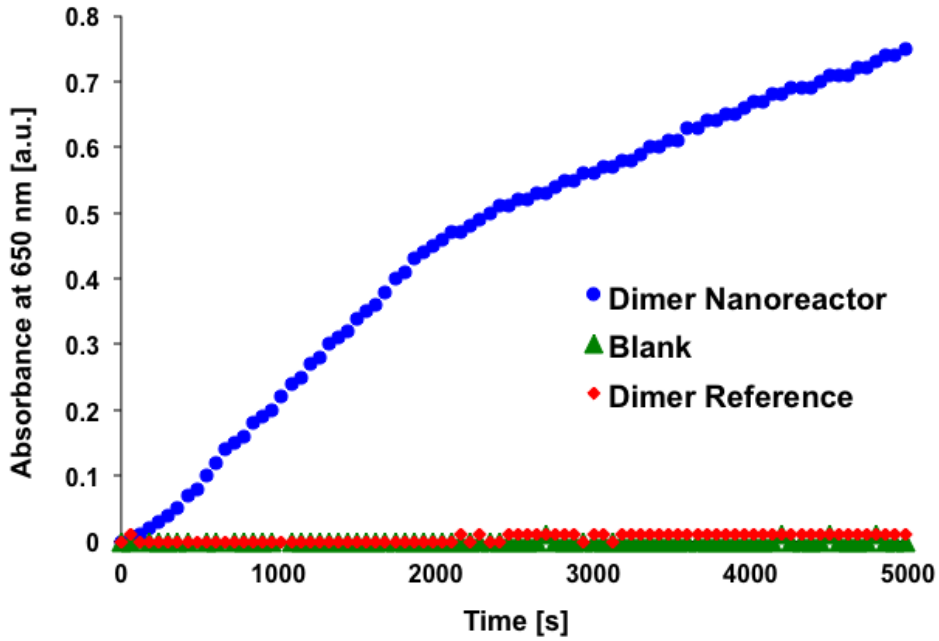

Figure 22: Change in TMB* absorbance as a function of time. Plots illustrate the activity of the enzyme pair GOx/HRP inside the DNA origami nanoreactor. The TMB-glucose substrate is used as a blank (black line) and the references are similarly prepared dimer without the avidin (and therefore the enzymes) (blue) and free enzymes in a solution with the substrate (green). The colour change of TMB is detected with spectrophotometer at wavelength of 650 nm [75].

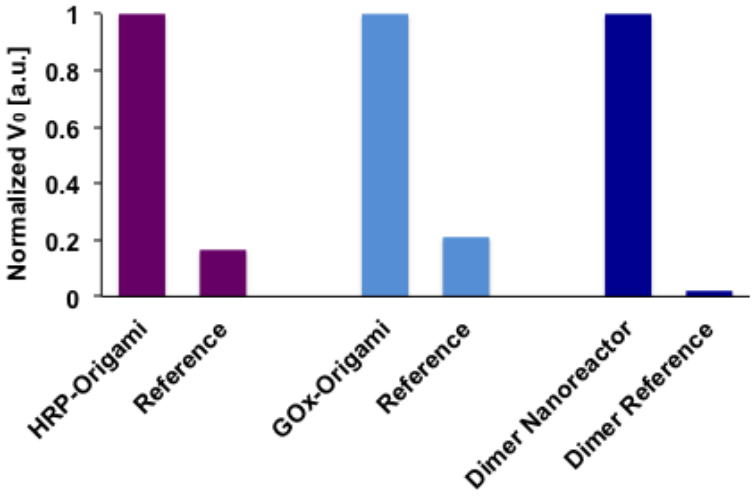

Figure 23: Initial rate of reactions (V_0) for enzymes attached to DNA units and for the assembled dimer nanoreactor. The initial rate of reaction for the sample is normalized to 1 in each case, and the performance of the sample is compared to a reference, which is fabricated and treated similarly but does not contain neutravidin modifications [75].

7 Summary and conclusions

In this study we demonstrated successfully the designing and production of DNA origami nanotubes and functionalisation of them with either HRP or GOx enzymes. We observed the enzymatic reactions in individual tubes by measuring the colour change of tetramethylbenzidine with a spectrophotometer. Finally, we demonstrated the construction of a modular multi-enzyme system attaching two origami units together via programmable DNA base pairing and observed the cascade reaction with spectrophotometric measurements. The hypothesis was that the reaction rate of the chosen catalyted reaction series increases if the catalytic enzymes are situated inside two origami tubes attached to each others compared to the situation where the origamis are separately in a solution. To prove this hypothesis correct, the results should be accompanied with samples including both versions of monomer origamis in same solution but not attached to each others. This was not done due to the limited time assigned to this project.

The reactor could be utilised as a nanoscale diagnostic tool, and modularity of the proposed system would further enable more complex reactions since the number of the units in the reactor is not limited. Each DNA origami unit can act as a modular building block hosting a chosen catalyst, or any other desired function, and the compartmentalisation of the enzymes could enhance the reaction rates especially in the case of larger molecules that are not able to diffuse through the walls of a DNA origami unit. These blocks can be further controllably assembled together in any desired order thus forming a defined-size tubular nanofactory with a tailored assembly line. In addition, these tubular DNA vessels could be used for transporting cargo or an incorporated functional device into cells either via virus [21] or lipid bilayer encapsulation [77] thus opening up countless opportunities for intriguing bionanotechnological applications.

The next step for developing the system would be to attach three functionalised origami units together instead of only two and demostrate a three-step enzymatic reaction. One logical addition would be adding β-galactosidase (β-Gal) into the third origami tube. β-Gal hydrolyses lactose to D-glucose and D-galactose. D-glucose can then be used as a substrate by GOx like previously described. Also, a workable and effective strategy to remove the excess of GOx enzyme should be found. The most straightforward option would be finding commercially available filter device for spin-filtering with convenient cut-off and pore size. Another option is using gel electrophoresis as a purification method. For this particular project this was found challenging because of samples' very low concentrations, but for more concentrated samples the method would be potential.

Fu *et al.* have studied the effect of the distance between the two enzymes, glucose oxidase and horseradish peroxidase, varying the spacing between 10 and 65 nm [53]. They discovered that the effect of the spacing to enzyme activity is significant. In this work the enzyme has three possible attachment locations inside one origami tube. Hence, the distance between the reaction sites (the distance between the enzymes GOx and HRP) can vary from 25 to 35 nm. In previous studies the enzymes have been on a plane or inside a small tube [73]. In our study the enzymes are

located inside two hollow tubes which are attached to each other after the assembly of enzymes. Since the diffusion of the H_2O_2 is crucial for the enzyme activity, the distance dependence studies should be repeated in this kind of partly closed structures.

According to Pinheiro *et al.* [39] the two major obstacles remaining for the growth of the field of DNA nanotechnology are the high cost of synthetic DNA and the relatively high error rate of self-assembly. In 2011 the total material costs for a new origami with M13mp18 scaffold were approximately 550 euros, with the price of 0.08 euros per base on 25 nmol scale. The synthesis is fully automated but because of side reactions and reaction errors accumulating with the length of the oligonucleotide, it requires purification steps, for instance chromatography techniques. Also, more understanding is required about the kinetics and thermodynamics of self-assembly of DNA structures and particularly, tools should be developed to analyse the defects occuring in complex DNA nanostructures [78]. Critics have argumented that the DNA origami structures often look pretty but only few have actual practical use. Proteins seem more natural and suitable choice for several tasks, such as drug delivery, and therefore competitive method, protein origamis, have been published [79].

Another obstacle for the growth of the usage of DNA origami method, and one of the major challenges during this thesis project, has been the difficulty to prepare the nanostructures in large enough concentrations. Stahl *et al.* propose to solve this problem with a new PEG-purification technique based on poly(ethylene glycol)-induced (PEG) depletion of species with high molecular weight. They claim the method to be applicable to a wide spectrum of DNA shapes and to achieve yields up to 97 %. With this method DNA objects could be prepared at concentrations up to solubility limit and even bringing DNA origamis into a solid phase. This new purification method is anticipated to further speed up the development of new types of applications for self-assembled DNA objects [80].

References

[1] Nangreave, J., Han, D., Liu, Y., Yan, H. DNA origami: a history and current perspective. *Current Opinion in Chemical Biology,* 2010, vol. 14, p. 608–615.

[2] Rothemund, P. W. K. Folding DNA to create nanoscale shapes and patterns. *Nature,* 2006, vol. 440, issue 16, p. 297–302.

[3] Linko, V., Dietz, H. The enabled state of DNA nanotechnology. *Current Opinion in Biotechnology,* 2013, vol. 24, p. 555–561.

[4] Ke, Y., Ong, L. L., Sun, W., Song, J., Dong, M., Shih, W. M., Yin, P. DNA brick crystals with prescribed depths. *Nature Chemistry,* 2014, vol. 6, p. 994–1002.

[5] Charoenphol, P., Bermudez, H. Design and application of multifunctional DNA nanocarriers for therapeutic delivery. *Acta Biomaterialia,* 2014, vol. 10, issue 4, p. 1683–1691

[6] Liu, Q., Song, C., Wang, Z.-G., Li, N., Ding, B. Precise organization of metal nanoparticles on DNA origami template. *Methods,* 2014, vol. 67, issue 2, p. 205–214.

[7] Nelson, D. L., Cox, M. M. *Lehninger Principles of Biochemistry,* 3rd ed., 2000, Worth Publishers, New York, 1152 p.

[8] Blackburn, G. M., Gait, M. J., Loakes, D., Williams, D. M. (Eds.). *Nucleic Acids in Chemistry and Biology,* 3rd ed., 2006, Cambridge, The Royal Society of Chemistry, 470 p.

[9] Eskelinen, A.-P. Nanoscale Assembly Using DNA and Electromagnetic Fields. Doctoral dissertation, 2013/139. Aalto University School of Science, Department of Applied Physics, Espoo, 104 p.

[10] Seeman, N. C. Nanomaterials based on DNA. *Annual Review of Biochemistry,* 2010, vol. 7, p. 65–87.

[11] Simmel, F. C., Dittmer, W. U. DNA Nanodevices. *Small,* 2005, vol. 1, issue 3, p. 284–299.

[12] Linko, V., Leppiniemi, J., Paasonen, S.-T., Hytönen, V. P., Toppari, J. J. Defined-size DNA triple crossover construct for molecular electronics: modification, positioning and conductance properties. *Nanotechnology,* 2011, vol. 22, 275610.

[13] Linko, V., Paasonen, S.-T., Kuzyk, A., Törmä, P., Toppari, J. J. Characterization of the Conductance Mechanisms of DNA Origami by AC Impedance Spectroscopy. *Small,* 2009, vol. 5, issue 21, p. 2382–2386.

[14] Linko, V., Toppari, J. J. Self-Assembled DNA-Based Structures for Nanoelectronics. *Journal of Self-Assembly and Molecular Electronics (SAME),* 2013, vol. 1, issue 1, p. 101–124.

[15] Linko, V. DNA-based applications in molecular electronics. Doctoral dissertation, 2011/2. University of Jyväskylä, Department of Physics, Jyväskylä, 120 p.

[16] Livshits, G. I., Stern, A., Rotem, D., Borovok, N., Eidelshtein, G., Migliore, A., Penzo, E., Wind, S. J., Di Felice, R., Skourtis, S. S., Cuevas, J. C., Gurevich, L., Kotlyar, A. B., Porath, D. Long-range charge transport in single G-quadruplex DNA molecules. *Nature Nanotechnology,* 2014, DOI: 10.1038/NNANO.2014.246

[17] Jena Image Library of Biological Macromolecules. `http://jenalib.fli-leibniz.de/image_library/DNA/DNA_models`

[18] Oligonucleotide Properties Calculator `http://www.basic.northwestern.edu/biotools/OligoCalc.html`

[19] Zuker, M. Mfold web server for nucleic acid folding and hybridization prediction. *Nucleic Acids Research,* 2003, vol. 31, issue 13, p. 3406–3415.

[20] Freitas, R. A. Jr. *Nanomedicine, Volume IIA: Biocompatibility.* Landes Bioscience, 2003, Texas, 348 p.

[21] Mikkilä, J., Eskelinen, A.-P., Niemelä, E. H., Linko, V., Frilander, M. J, Törmä, P., Kostiainen, M. A. Virus-Encapsulated DNA Origami Nanostructures for Cellular Delivery. *Nano Letters,* 2014, vol. 14, issue 4, p. 2196–2200 .

[22] Langecker, M., Arnaut, V., List, J., Simmel, F. C. DNA nanostructures interacting with lipid bilayer membranes. *Accounts of chemical research,* 2014, vol. 47, p. 1807–1815.

[23] Wei, B., Dai, M., Yin, P. Complex shapes self-assembled from single-stranded DNA tiles. *Nature,* 2012, vol. 485, p. 623–627.

[24] Ke, Y., Ong, L. L., Shih, W. M., Yin, P. Three-dimensional structures self-assembled from DNA bricks. *Science,* 2012, vol. 338, p. 1177–1183.

[25] Endo, M., Yang, Y., Sugiyama, H. DNA origami technology for biomaterials applications. *Biomaterials Science,* 2013, vol. 1, p. 347–360.

[26] Högberg, B., Liedl, T., Shih, W. M. Folding DNA origami from a double-stranded source of scaffold. *Journal of American Chemical Society,* 2009, vol. 131, issue 26, p. 9154–9155.

[27] Pound, E., Ashton, J. R., Becerril, H. A., Woolley, A. T. Polymerase chain reaction based scaffold preparation for the production of thin, branched DNA origami nanostructures of arbitrary sizes. *Nano Letters,* 2009, vol. 9, issue 12, p. 4302–4305.

[28] Tørring, T., Voigt, N. V., Nangreave, J., Yan, H., Gothelf, K. V. DNA origami: a quantum leap for self-assembly of complex structures. *Chemical Society Reviews,* 2011, vol. 40, p. 5636–5646.

[29] Castro, C. E., Kilchherr, F., Kim, D.-N., Shiao, E. L., Wauer, T., Wortmann, P., Bathe, M., Dietz, H. A primer to scaffolded DNA origami. *Nature Methods*, 2011, vol. 8, issue 3, p. 221–229.

[30] Eskelinen, A.-P., Kuzyk, A., Kaltiaisenaho, T. K., Timmermans, M. Y., Nasibulin, A. G., Kauppinen, E. I., Törmä, P. Assembly of Single-Walled Carbon Nanotubes on DNA-Origami Templates through Streptavidin-Biotin Interaction. *Small,* 2011, vol. 7, p. 746–750.

[31] Ke, Y., Voigt, N. V., Gothelf, K. V., Shih, W. M. Multilayer DNA origami packed on hexagonal and hybrid lattices. *Journal of American Chemical Society,* 2011, vol. 134, p. 1770–1774.

[32] Dietz, H., Douglas, S. M., Shih, W. M. Folding DNA into twisted and curved nanoscale shapes. *Science,* 2009, vol. 325, p. 725–730.

[33] Gross, M. DNA nanotechnology gets real. *Current Biology*, 2013, vol. 23, p. R95–R98.

[34] Sobczak, J.-P. J., Martin, T. G., Gerling, T., Dietz, H. Rapid folding of DNA into nanoscale shapes at constant temperature. *Science,* 2012, vol. 338, p. 1458–1461.

[35] Lin, C., Perrault, S. D., Kwak, M., Graf, F., Shih, W. M. Purification of DNA-origami nanostructures by rate-zonal centrifugation. *Nucleic Acids Research,* 2013, vol. 41, issue 2, e40.

[36] Lo, P. K., Metera, K. L., Sleiman, H. F. Self-assembly of three-dimensional DNA nanostructures and potential biological applications. *Current Opinion in Chemical Biology,* 2010, vol. 14, p. 597–607.

[37] Jungmann, R., Scheible, M., Kuzyk, A., Pardatscher, G., Castro, C. E., Simmel, F. C. DNA origami-based nanoribbons: assembly length distribution, and twist. *Nanotechnology,* 2011, vol. 22, issue 27, 275301.

[38] Douglas, S. M., Dietz, H., Liedl, T., Högberg, B., Graf, F., Shih, W. M. Self-assembly of DNA into nanoscale three-dimensional shapes. *Nature,* 2009, vol. 459, p. 414–418.

[39] Pinheiro, A. V., Han, D., Shih, W. M., Yan, H. Challenges and opportunities for structural DNA nanotechnology. *Nature Nanotechnology,* 2011, vol. 6, p. 763–772.

[40] Zhao, Z., Liu, Y., Yan, H. Organizing DNA origami tiles into larger structures using preformed scaffold frames. *Nano Letters,* 2011, vol. 11, p. 2997–3002.

[41] Schüller, V. J., Heidegger, S., Sandholzer, N., Nickels, P. C., Suhartha, N. A., Endres, S., Bourquin, C., Liedl, T. Cellular immunostimulation by CpG sequence-coated DNA origami structures. *ACS Nano,* 2011, vol. 5, issue 12, p. 9696–9702.

[42] Li, J., Pei, H., Zhu, B., Liang, L., Wei, M., He, Y., Chen, N., Li, D., Huang, Q., Fan, C. Self-assembled multivalent DNA nanostructures for noninvasive intracellular delivery of immunostimulatory CpG oligonucleotides. *ACS Nano,* 2011, vol. 5, issue 12, p. 8783–8789.

[43] Kuzyk, A., Laitinen, K. T., Törmä, P. DNA origami as a nanoscale template for protein assembly. *Nanotechnology,* 2009, vol. 20, issue 23, 235305.

[44] Eskelinen, A.-P., Rosilo, H., Kuzyk, A., Törmä, P., Kostiainen, M. A. Controlling the formation of DNA origami structures with external signals. *Small,* 2012, vol. 8, issue 13 p. 2016–2020.

[45] Eskelinen, A.-P., Moerland, R. J., Kostiainen, M. A., Törmä, P. Self-assembled silver nanoparticles in a bow-tie antenna configuration. *Small,* 2014, vol. 10, issue 6, p. 1057–1062.

[46] Bellot, G., McClintock, M. A., Chou, J. J., Shih, W. M. DNA nanotubes for NMR structure determination of membrane proteins. *Nature Protocols,* 2013, vol. 8, issue 4, p. 755–770.

[47] Douglas, S. M., Chou, J. J., Shih, W. M. DNA-nanotube-induced alignment of membrane proteins for NMR structure determination. *PNAS,* 2007, vol. 104, issue 16, p. 6644–6648.

[48] Wei, R., Martin, T. G., Rant, U., Dietz, H. DNA Origami Gatekeepers for Solid-State Nanopores. *Angewandte Chemie,* 2012, vol. 124, p. 4948–4951.

[49] Plesa, C., Ananth, A. N., Linko, V., Gülcher, C., Katan, A. J., Dietz, H., Dekker, C. Ionic permeability and mechanical properties of DNA origami nanoplates on solid-state nanopores. *ACS Nano,* 2014, vol. 8, issue 1, p. 35–43.

[50] Kuzyk, A., Schreiber, R., Fan, Z., Pardatscher, G., Roller, E.-M., Högele, A., Simmel, F. C., Govorov, A. O., Liedl, T. DNA-based self-assembly of chiral plasmonic nanostructures with tailored optical response. *Nature,* 2012, vol. 483, p. 311–314.

[51] Derr, N. D., Goodman, B. S., Jungmann, R., Leschziner, A. E., Shih, W. M., Reck-Peterson, S. L. Tug-of-war in motor protein ensembles revealed with a programmable DNA origami scaffold. *Science,* 2012, vol. 338, issue 6107, p. 662–665.

[52] Simmel, F. C. DNA-based assembly lines and nanofactories. *Current Opinion in Biotechnology,* 2012, vol. 23, p. 516–521.

[53] Fu, J., Liu, M., Liu, Y., Woodbury, N. W., Yan, H. Interenzyme substrate diffusion for an enzyme cascade organized on spatially addressable DNA nanostructures. *Journal of the American Chemical Society,* 2012, vol. 134, p. 5516–5519.

[54] Kuzyk, A., Yurke, B., Toppari, J., Linko, V., Törmä, P. Dielectrophoretic trapping of DNA origami. *Small,* 2008, vol. 4, issue 4, p. 447–450.

[55] Kuzuya, A., Watanabe, R., Hashizume, M., Kaino, M., Minamida, S., Kameda, K., Ohya, Y. Precise structure control of three-state nanomechanical DNA origami devices. *Methods,* 2014, vol. 67, p. 250–255.

[56] Douglas, S. M., Bachelet, I., Church, G. M. A logic-gated nanorobot for targeted transport of molecular payloads. *Science,* 2012, vol. 335, issue 6070, p. 831–834.

[57] Torelli, E., Marini, M., Palmano, S., Piantanida, L., Polano, C., Scarpellini, A., Lazzarino, M., Firrao, G. A DNA origami nanorobot controlled by nucleic acid hybridization. *Small,* 2014, vol. 10, issue 14, p. 2918–2926.

[58] van Dongen, S. F. M., Nallani, M., Cornelissen, J. J. L. M., Nolte, R. J. M., van Hest, J. C. M. A three-enzyme cascade reaction through positional assembly of enzymes in a polymersome nanoreactor. *Chemistry A European Journal,* 2009, vol. 15, p. 1107–1114.

[59] Peters, R. J. R. W., Louzao, I., van Hest, J. C. M. From polymeric nanoreactors to artificial organelles. *Chemical Science,* 2012, vol. 3, p. 335–342.

[60] Kuiper, S. M., Nallani, M., Vriezema, D. M., Cornelissen, J. J. L. M., van Hest, J. C. M., Nolte, R. J. M., Rowan, A. E. Enzymes containing porous polymersomes as nano reaction vessels for cascade reactions. *Organic & Biomolecular Chemistry,* 2008, vol. 6, p. 4315–4318.

[61] Fu, J., Yang, Y. R., Johnson-Buck, A., Liu, M., Liu, Y., Walter, N. G., Woodbury, N. W., Yan, H. Multi-enzyme complexes on DNA scaffolds capable of substrate channelling with an artificial swinging arm. *Nature Nanotechnology,* 2014, vol. 9, p. 531–536.

[62] Li, K., Nguyen, H. G., Lu, X., Wang, Q. Viruses and their potential in bioimaging and biosensing applications. *Analyst,* 2010, vol. 135, p. 21–27.

[63] Liljeström, V., Mikkilä, J., Kostiainen, M. A. Self-assembly and modular functionalization of three-dimensional crystals from oppositely charged proteins. *Nature Communications,* 2014, vol. 5, issue 4445.

[64] Cardinale, D., Carette, N., Michon, T. Virus scaffolds as enzyme nano-carriers. *Trends in Biotechnology,* 2012, vol. 30, issue 7, p. 369–376.

[65] Vriezema, D. M., Garcia, P. M. L., Oltra, N. S., Hatzakis, N. S., Kuiper, S. N., Nolte, R. J. M., Rowan, A. E., van Hest, J C. M. Positional assembly of enzymes in polymersome nanoreactors for cascade reactions. *Angewandte Chemie, Int. Ed.* 2007, vol. 46, p. 7378–7382.

[66] Pan, X., Fan, Z., Chen, W., Ding, Y., Luo, H., Bao, X. Enhanced ethanol production inside carbon-nanotube reactors containing catalytic particles. *Nature Materials,* 2007, vol. 6, p. 507–511.

[67] Chamberlain, T. W., Earley, J. H., Anderson, D. P., Khlobystov, A. N., Bourne, R. A. Catalytic nanoreactors in continuous flow: hydrogenation inside single-walled carbon nanotubes using supercritical CO_2. *Chemical Communications,* 2014, vol. 50, p. 5200–5202.

[68] Avnir, D., Coradin, T., Lev, O., Livage, J. Recent bio-applications of sol-gel materials. *Journal of Materials Chemistry,* 2006, vol. 16, p. 1013–1030.

[69] Li, Z., Zhang, Y., Su, Y., Ouyang, P., Ge, J., Liu, Z. Spatial co-localization of multi-enzymes by inorganic nanocrystal–protein complexes. *Chemical Communications,* 2014, vol. 50, p. 12465–12468.

[70] Fu, Q., Li, W.-X., Yao, Y., Liu, H., Su, H.-Y., Ma, D., Gu, X.-K., Chen, L., Wang, Z., Zhang, H., Wang, B., Bao, X. Interface-Confined Ferrous Centers for Catalytic Oxidation. *Science,* 2010, vol. 328, p. 1141–1144.

[71] RCSB Protein Data Bank, `http://www.rcsb.org/pdb/home/home.do`

[72] Müller, J., Niemeyer, C. M. DNA-directed assembly of artificial multienzyme complexes. *Biochemical and Biophysical Research Communications,* 2008, vol. 377, p. 62–67.

[73] Fu, Y., Zeng, D., Chao, J., Jin, Y., Zhang, Z., Liu, H., Li, D., Ma, H., Huang, Q., Gothelf, K. V., Fan, C. Single-Step Rapid Assembly of DNA Origami Nanostructures for Addressable Nanoscale Bioreactors. *Journal of the American Chemical Society,* 2013, vol. 135, p. 696–702.

[74] Douglas, S. M., Marblestone, A. H., Teerapittayanon, S., Vazquez, A., Church, G. M., Shih, W. M. Rapid prototyping of 3D DNA-origami shapes with caDNAno. *Nucleic Acids Research,* 2009, vol. 37, issue 2, p. 5001–5006.

[75] Linko, V., Eerikäinen, M., Kostiainen, M. A. A modular DNA origami-based enzyme cascade nanoreactor. *Chemical Communications,* under review.

[76] Hung, A. M., Micheel, C. M., Bozano, L. D., Osterbur, L. W., Wallraff, G. M., Cha, J. N. Large-area spatially ordered arrays of gold nanoparticles directed by lithographically confined DNA origami. *Nature Nanotechnology,* 2010, vol. 5, p. 121–126.

[77] Perrault, S. D., Shih, W. M. Virus-inspired membrane encapsulation of DNA nanostructures to achieve *in vivo* stability. *ACS Nano,* 2014, vol. 8, issue 5, p. 5132–5140.

[78] Wagenbauer, K. F., Wachauf, C. H., Dietz, H. Quantifying quality in DNA self-assembly. *Nature Communications,* 2014, vol. 5, issue 3691.

[79] Gradišar, H, Božič, S., Doles, T., Vengust, D., Hafner-Bratkovič, I., Mertelj, A., Webb, B., Šali, A., Klavžar, S., Jerala, R. Design of a single-chain polypeptide tetrahedron assembled from coiled-coil segments. *Nature Chemical Biology,* 2013, vol. 9, p. 362–366.

[80] Stahl, E., Martin, T. G., Praetorius, F., Dietz, H. Facile and scalable preparation of pure and dense DNA origami solutions. *Angewandte Chemie,* 2014, vol. 126, DOI: 10.1002/ange.201405991.

A Hexagonal tube design

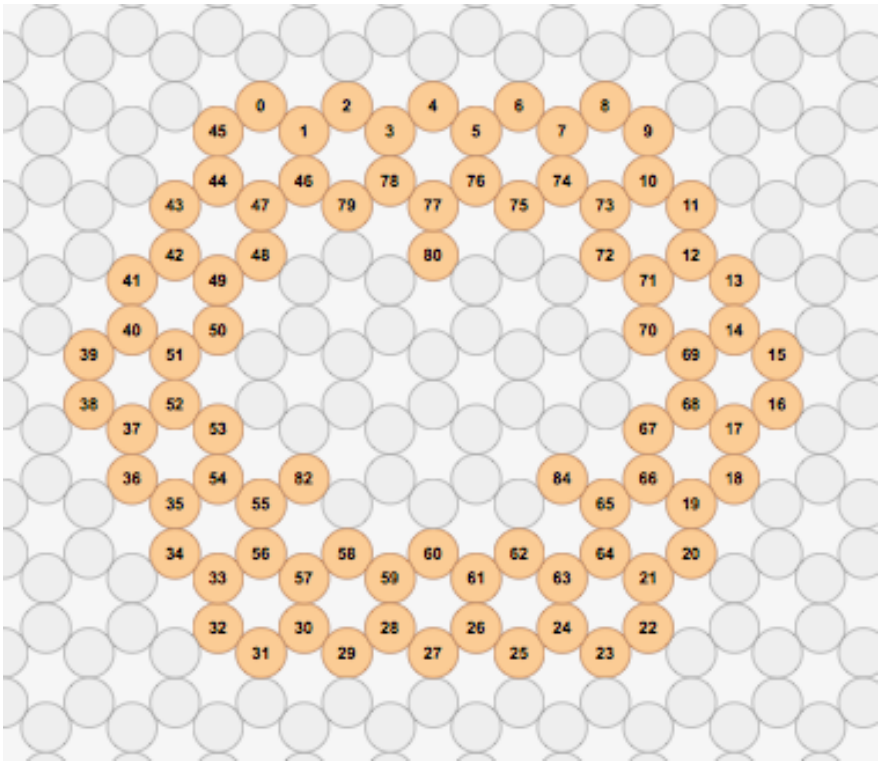

Figure A1: caDNAno design of the hexagonal tube. The circles with numbers 80, 82 and 84 indicate the positions of the biotinylated strands and therefore the attachment sites for neutravidin molecules.

B Transmission electron microscope images

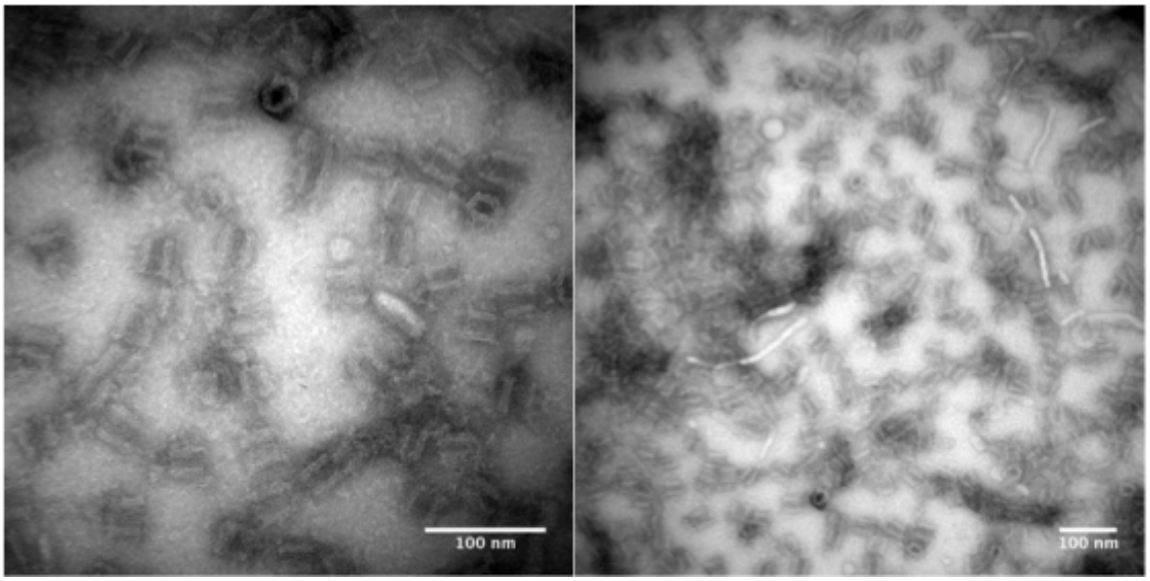

Figure B1: TEM images of DNA origami tubes. The scale bars are 100 nm.

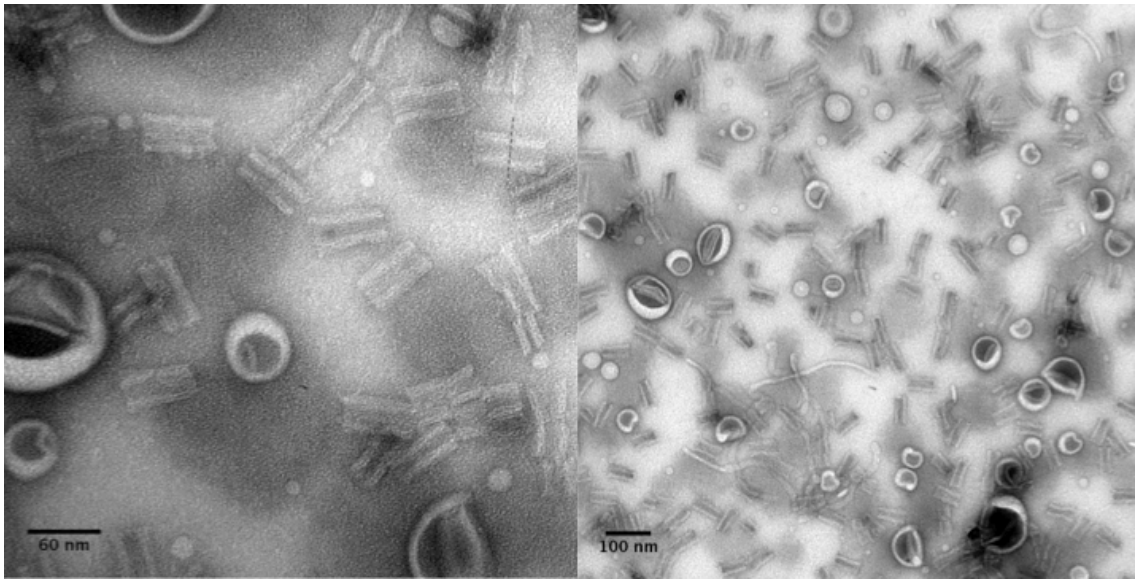

Figure B2: TEM images of DNA origami dimers. The scale bars are 60 nm (left) and 100 nm (right).

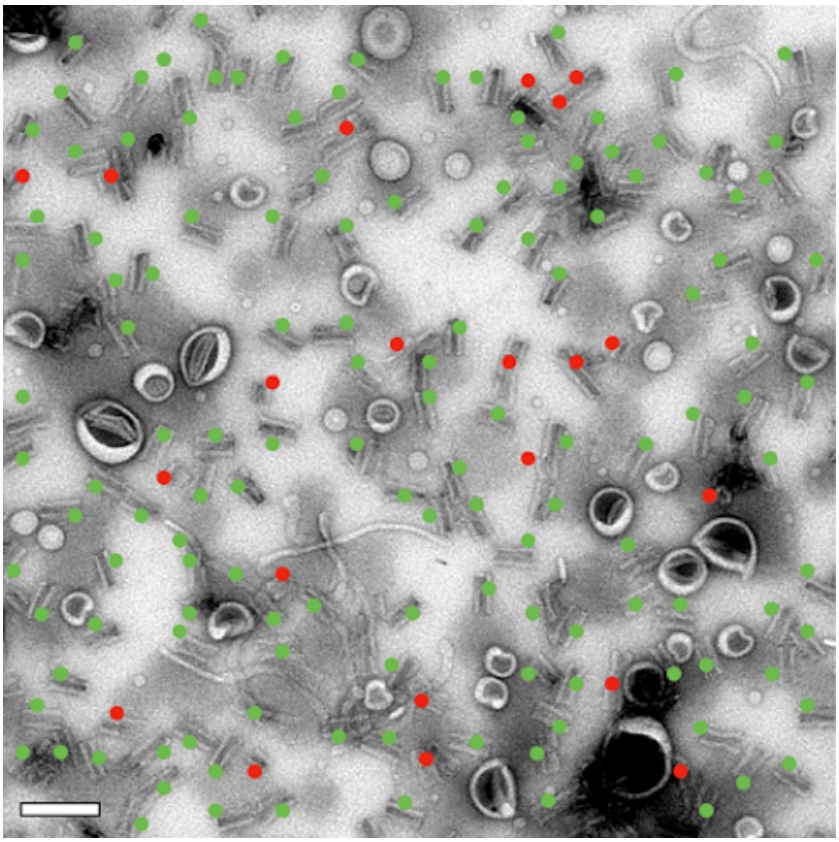

Figure B3: TEM image of DNA origami dimers. Correctly assembled dimer nanoreactors are marked with green dots and incorrect ones with red dots. the yield is approximated to be 86 %. The scale bar is 100 nm.

C Sequence maps of hexagonal tube origami

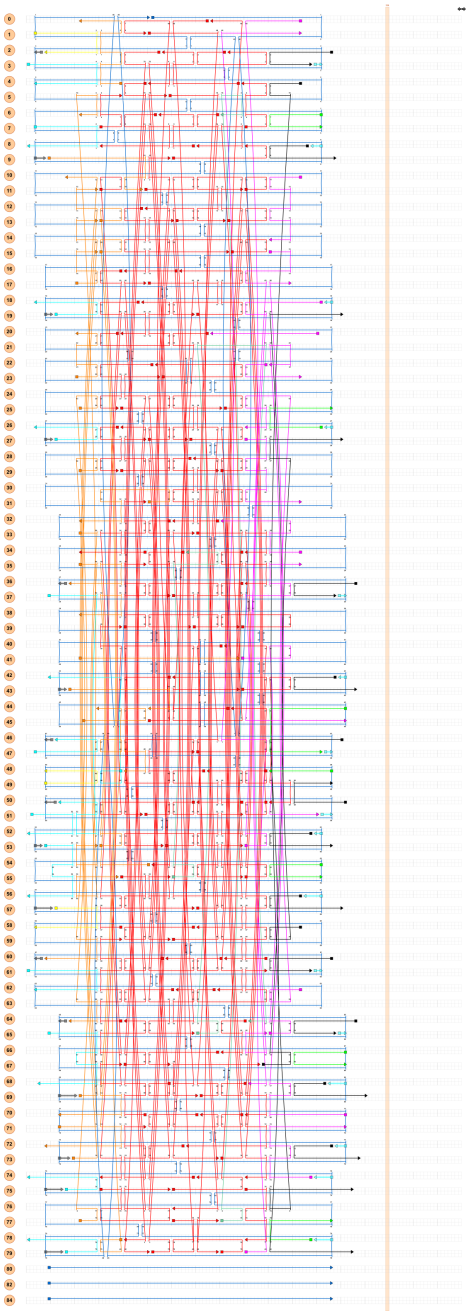

Figure C1: Sequence map of DNA scaffold and staple strands of the hexagonal tube origami shown with connecting strands (black and turqoise). Origamis with connecting strands on the left side and origamis with connecting strands on the right side are folded separately and combined afterwards to form dimers.

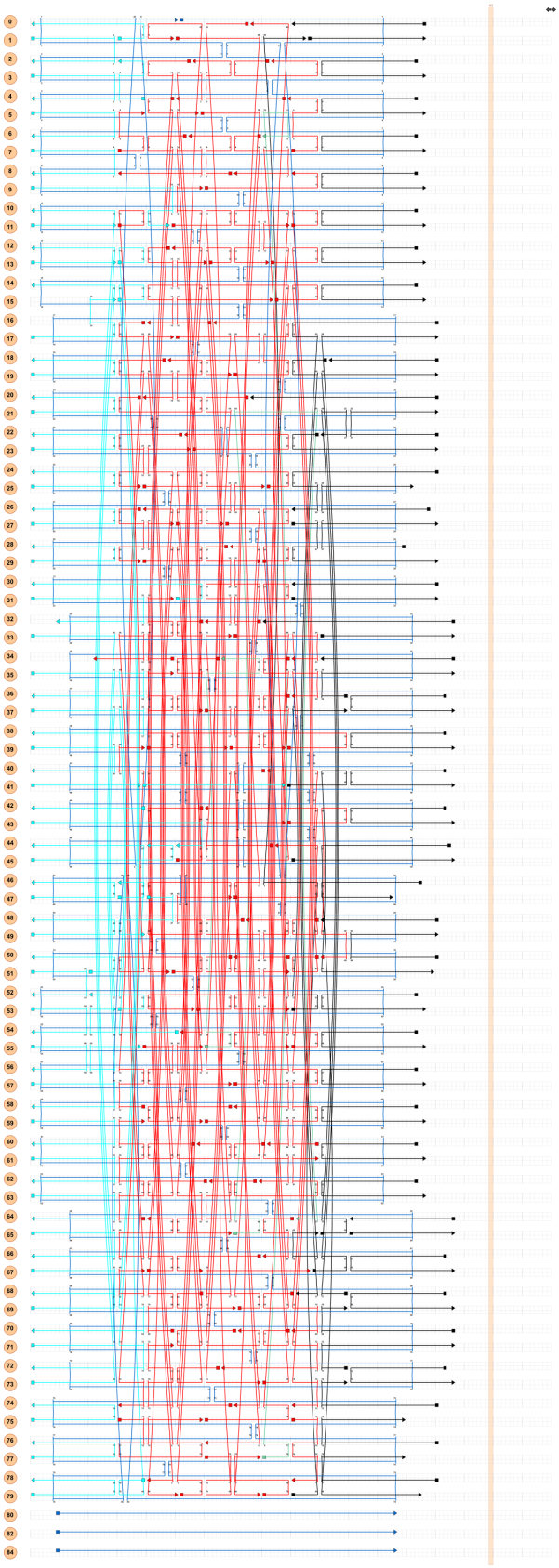

Figure C2: Sequence map of DNA scaffold and staple strands of the hexagonal tube origami shown with the polyT-strands. PolyT-overhangs are used to passivate the other end of the tube to inhibit the formation of multimers.